# WIDMANSTÄTTEN FERRITE AND BAINITE
# IN
# ULTRA HIGH STRENGTH STEELS

*By*

ASHRAF ALI

*Hughes Hall*

*A dissertation submitted for the fulfillment*
*of the degree of*

DOCTOR OF PHILOSOPHY

*at the University of Cambridge*

January, 1991

◇ To *Farhan, Hina, Nida and Faizan*

*" Science means simply the aggregate of the recipes that are always successful.*
*All the rest is li*<sub>e</sub>*rature"*

Paul Valŕy [1871-1945]

*Analects* vol. 14 of Collected Works ed. J. Matthews, 1970 (London: Routledge & Kegan Paul)

i

## ACKNOWLEDGEMENTS

I greatly acknowledge my wife, Mehr, for her moral support during the period of my research. I also express my gratitude to my parents for their constant encouragement in time of need. Last but not least I must thanks my son for his constant interest in the number of pages of the thesis.

*Ashraf Ali*

*ABSTRACT*

The microstructural, thermodynamic and kinetic aspects of Widmanstätten ferrite and bainite in steels have been studied with the aim of providing a better understanding of the mechanisms of phase transformation. The thesis begins with a review of the published literature on the physical metallurgy of steels, concentrating whenever possible, on the aspects important in the modelling of microstructures. This is followed by an experimental study of bainite in steels where the precipitation of carbides is sluggish. The results confirm the hypothesis that bainite grows without diffusion, although any excess carbon in the bainitic ferrite subsequently partitioned into the residual austenite.

The tempering of mixed microstructures of bainitic ferrite and austenite was found to cause changes in the shape of the originally lenticular bainite platelets, towards a more rounded microstructure. Prolonged annealing also led to the coalescence of adjacent platelets, until the austenite decomposed into cementite and ferrite. In steels with molybdenum, the cementite eventually transformed to alloy carbides.

Controlled experiments designed to classify the contradictory published data confirmed that the rate of bainite transformation increases as austenite grain size is reduced. Some spectacular microstructures of commercial significance were generated by decorating the austenite grain surfaces with thin layers of allotriomorphic ferrite in order to force the intragranular nucleation of Widmanstätten ferrite or bainite on minute quantities of oxide particles.

The process of Widmanstätten ferrite nucleation was studied using thermodynamic and kinetic modelling; both new experimental data and the analysis of published results indicate a displacive mechanism in which carbon redistributes during both nucleation and growth. On the other hand, the growth of bainite sheaves appears to occur at a rate much faster then expected from diffusion-controlled growth theory. This, and other experiments on the reverse transformation of bainitic ferrite into austenite, have all been found to be consistent with the model in which bainite is said to grow by a diffusionless mechanism.

# CONTENTS

## Chapter 1: Aspects of Displacive Phase Transformations in High Strength Steels

## Chapter 2: Reaustenitisation

## Chapter 3: Experimental: Techniques and Procedures

## Chapter 4: Study of the Bainite Transformation Using Dilatometry

## Chapter 5: Tempering of Bainite in Fe-C-Si-Mn-Mo Steel

## Chapter 6: Effect of Austenitisation Temperature on Bainite Formation

## Chapter 7: Intragranular Nucleation of Bainite Sheaves

## Chapter 8: Aspects of the Nucleation of Widmanstätten Ferrite Plates and Bainite Sheaves

# Chapter 9: The Growth of Widmanstätten Ferrite Plates and Bainite Sheaves

# Chapter 10: On the Formation of Intragranular Widmanstätten Ferrite Plates in Ultra High Strength Steels

# Chapter 11: Reaustenitisation in High Hardenability Steels

NOMENCLATURE AND ABBREVIATIONS

| | |
|---|---|
| $Ae_3$ | Upper temperature limit of the $\alpha + \gamma$ phase field at equilibrium |
| $Ae_3'$ | Upper temperature limit of the $\alpha + \gamma$ phase field at paraequilibrium |
| $Ae_1$ | Lower temperature limit of the $\alpha + \gamma$ phase field at paraequilibrium |
| $Ae_1'$ | Lower temperature limit of the $\alpha + \gamma$ phase field at equilibrium |
| $a_{Fe}^{\alpha}$ | Activity of iron in ferrite. |
| $a_{Fe}^{\gamma}$ | Activity of iron in austenite |
| $\alpha$ | Ferrite |
| $\alpha_a$ | Allotriomorphic ferrite |
| $\alpha_b$ | Bainitic ferrite |
| $\alpha_w$ | Widmanstätten ferrite |
| $\alpha'$ | Martensite |
| $a_{\gamma_o}$ | Lattice parameter of austenite at the reaction temperature before the reaction, Å |
| $a_{\gamma}$ | Lattice parameter of austenite at the reaction temperature at any stage of the reaction, Å |
| $a_{\alpha_o}$ | Lattice parameter of ferrite at ambient temperature (25 °C), Å |
| $a_{\alpha}$ | Lattice parameter of ferrite at reaction temperature, Å |
| $B_S$ | The temperature at which bainite first observed to form, in °C |
| $\overline{D}$ | Weighted average diffusivity of carbon in austenite |
| $E^{str}$ | Strain energy per unit volume |
| $e_{\alpha,\gamma}$ | Linear thermal expansion coefficient of ferrite and austenite respectively, °C$^{-1}$ |
| $G_1$ | Stored energy of Widmanstätten ferrite *i.e.,* 50 J mol$^{-1}$ |
| $G_2$ | Stored energy of bainite *i.e.,* 400 J mol$^{-1}$ |
| $G_{max}$ | Maximum free energy required for the nucleation of Widmanstätten ferrite in J mol$^{-1}$ |
| $\Delta G^{\gamma \to \gamma' + \alpha}$ | Driving force required for the ferrite from austenite with shear in J mol$^{-1}$ |
| $\Delta G$ | Change in Gibb's free energy, J mol$^{-1}$ K$^{-1}$ |
| $G_N$ | Minimum amount of free energy required for the nucleation of Widmanstätten ferrite irrespective of the chemical composition of steels in J mol$^{-1}$ |
| $\Delta G^{\gamma \to \alpha_s}$ | Free energy change accompanying the formation of ferrite in J mol$^{-1}$ with the same carbon content as austenite in J mol$^{-1}$ |

| | |
|---|---|
| $\Delta G^{\gamma \rightarrow \alpha}$ | Free energy change from austenite to ferrite transformation in pure iron, in J mol$^{-1}$ |
| $\Delta G_o^*$ | Activation energy in the absence of applied stress |
| $\Delta G^{chem}$ | Chemical driving force, J mol$^{-1}$ |
| $\Delta G^*$ | Activation energy term of isothermal nucleation theory in J mol$^{-1}$K$^{-1}$ |
| $\Delta G_v^o$ | Maximum volume free energy change accompanying the formation of nucleus in a large amount of matrix phase in J mol$^{-1}$K$^{-1}$ |
| IPS | Invariant plane strain |
| $L$ | Length of the specimen prior to the transformation, mm |
| $\Delta L$ | Length change due to transformation, mm |
| $M_S$ | Martensite start temperature, in $^o$C |
| $N$ | Steady state nucleation rate |
| NP-LE | Negligible partitioning local equilibrium |
| P-LE | Partitioning local equilibrium |
| $V_\alpha$ | Volume fraction of ferrite transformed |
| $\gamma$ | Austenite |
| $T_\gamma$ | Isothermal reaustenitisation temperature in $^o$C |
| $\sigma$ | Interfacial energy per unit area |
| $T_0$ | Temperature at which stress-free austenite and ferrite of the same composition have identical free energies, $^o$C |
| $T_0'$ | Same as $T_0$ except taking stored energy 400 J mol$^{-1}$ of bainite, $^o$C |
| $r$ | Radius of spherical nucleus |
| $r^*$ | Radius of critical nucleus |
| $R$ | Universal gas constant |
| $S$ | Carbon locked up in ferrite, at. % |
| $T$ | Reaction temperature in $^o$C |
| $\tau_s$ | Incubation period, s |
| $\tau_o$ | Shear stress required to move an array of n dislocations |
| $\nu$ | Pre-exponential attempt frequency factor of nucleation theory |
| $\rho_A$ | Density of atoms in the closed packed plane |
| $\overline{x}$ | Average carbon content in the steel, at. %, |
| $x_{Si}$ | Average silicon content in the steel, at.% |
| $x_{Mn}$ | Average manganese content in the steel, at.% |
| $x_{Mo}$ | Average molybdenum content in the steel, at.% |
| $x_\gamma$ | Carbon content of residual austenite at any stage of the reaction, at.% |
| $\overline{x}$ | Average carbon concentration of the alloy |

| | |
|---|---|
| $x_{max}$ | Maximum level of carbon permitted in ferrite for a specified carbon concentration in the austenite at the interface |
| $x^{\gamma\alpha}$ | Equilibrium concentration of carbon in austenite at austenite/ferrite interface |
| $x^{\alpha\gamma}$ | Equilibrium concentration of carbon in ferrite at austenite/ferrite interface |
| $W_S$ | The highest temperature at which Widmanstätten ferrite forms in a detectable amount, in °C |

# Chapter 1
# ASPECTS OF DISPLACIVE PHASE TRANSFORMATIONS IN HIGH-STRENGTH STEELS

There is a complex series of reconstructive and displacive transformation products formed as a result of the decomposition of austenite during transformation at temperatures below $Ae_3$, when various alloying elements are added to pure iron. These microstructures vary not just in morphology, but in phase composition, structure and thermodynamic stability. The microstructure of low-alloy steels can contain allotriomorphic ferrite, Widmanstätten ferrite, acicular ferrite, bainite, martensite and retained austenite, depending upon the transformation temperature, alloy composition and cooling rate etc.

The austenite to ferrite ($\gamma \rightarrow \alpha$) transformation in low-alloy steels is a topic of vital concern to metallurgists and considerable attention has been given in recent years to the elucidation of the mechanisms which govern the displacive decomposition of austenite to ferrite [Bhadeshia, 1981a; 1987a].

In the following section some of the basic concepts which govern the displacive transformation mechanism are discussed. A comparative study of the reconstructive and displacive transformation mechanisms is presented and finally, various decomposition products formed by both reconstructive and displacive transformation mechanisms are described.

## 1.1 Reconstructive, Martensitic and Displacive Transformations

Based on the features exhibited by a transformation product, such as morphology, chemical composition and change in the shape of the transformed region, the $\gamma \rightarrow \alpha$ decomposition reaction can be classified into three main groups [Christian, 1975a; Bhadeshia, 1985a]. *Reconstructive transformations* are those in which the interface advances by the thermally activated uncoordinated movement of atoms across the interface (the atoms behave in the manner of civilians). That is they move independently of each other and in an apparently random manner.

For a reconstructive transformation, it is evident (Fig. 1.1) that the product phase can (although it need not) be of a different composition from the parent phase. In addition, there has been much mixing up of atoms during transformation and there is no atomic correspondence between the parent and product lattices. Because the transformation involves a reconstruction of the parent lattice, atoms are able to diffuse and mix in such a way that the invariant-plane strain (IPS) shape
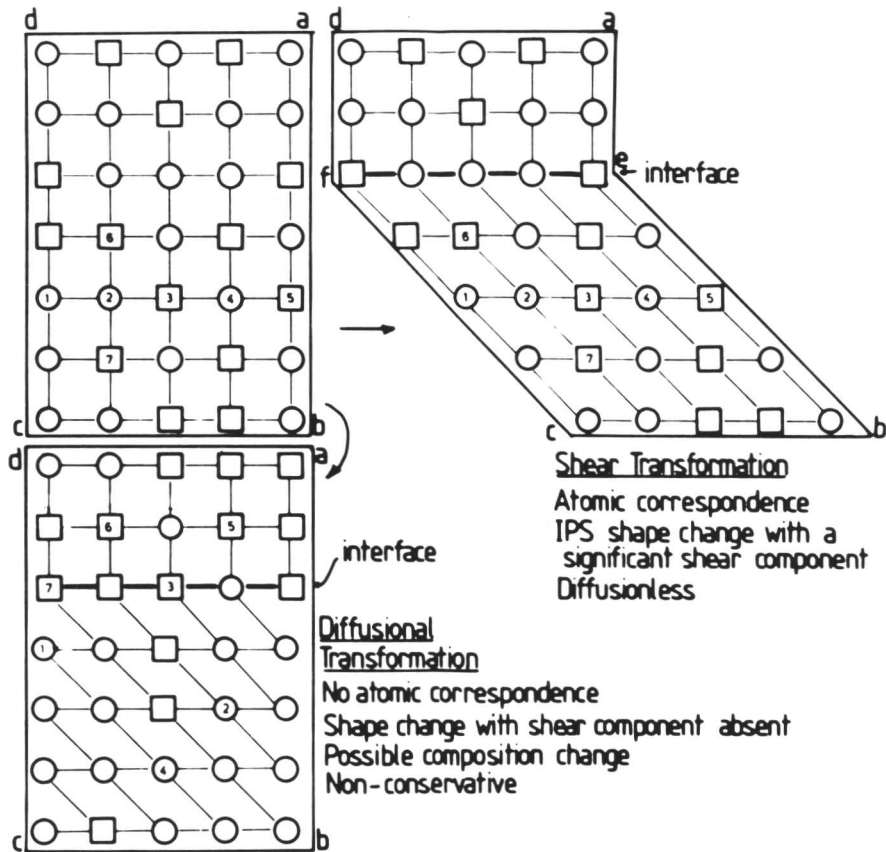
Fig. 1.1: *Schematic illustration of the mechanism of reconstructive and martensitic transformations in a substitutionally alloyed materials. The lines joining "atoms" connects corresponding direction of the parent and product lattices [Bhadeshia, 1987b].*

deformation (and its attendant strain energy) does not arise. The diffusion necessary to accomplish the lattice change without the strain accompanying the coordinated movement of atoms is called *reconstructive diffusion* [Bhadeshia, 1985a], and it is necessary even when reconstructive reactions occur in a pure element. Reconstructive transformations can be regarded as simultaneous transformation and recrystallisation, the recrystallisation part involving reconstructive diffusion.

*Martensitic* or military transformations are reactions in which the rearrangement of atoms takes place in an orderly, disciplined manner, the transfer being diffusionless. Since the pattern in which the atoms of the parent crystal arranged nevertheless changes in a way that is consistent with the change in crystal structure, it follows that there must be a physical change in the macroscopic shape of the parent crystal during transformation. This shape change in the transformed region can be observed, if a pre-polished specimen is allowed to transform to a martensitic transformation. This particular shape change is known as *invariant-plane strain*§, and it has a shear component as well as with the dilatation component [Christian, 1958]. Fig. 1.1 shows that in a martensitic transformation, labelled rows of atoms in the parent crystal remain in the correct sequence in the martensite lattice, despite transformation. As there is no mixing up of atoms during transformation, it is possible to suggest that a particular atom of the martensite originated from a corresponding particular atom in the parent crystal. This property may be expressed by stating that there exists an atomic correspondence between the parent and product lattices.

In interstitially alloyed materials, the substitutional lattice can transform without diffusion while the interstitials may diffuse [Christian, 1962], this is *displacive transformation*. The diffusion of interstitials has no influence on the shape change accompanying transformation so that the macroscopic characteristics of martensite are retained. Only a partial atomic correspondence (between atoms on the substitutional lattices) exists between the parent and product lattices. Martensitic transformations can be regarded as a *diffusionless* subset of displacive transformations [Cohen *et al.* 1979].

## 1.2 Comparison between Martensitic and Displacive Transformations

Martensitic reactions are always interface-controlled whereas displacive or reconstructive transformations need not be; their rate can be controlled by diffusion

§ see also section 1.6 for details.

in the parent phase. In both displacive and martensitic transformations, the product phase always has thin-plate morphology since this minimizes the strain energy associated with the shape deformation [Bilby and Christian, 1956].

In martensitic or displacive transformations the structure of the interface necessarily has to be coherent or semi-coherent in order to ensure glissile interfaces. The kinetics, however may be controlled by either the nucleation or the growth rate. The *experimental criterion which best distinguishes between martensitic or displacive transformations from reconstructive transformations is the observation of whether or not there is an IPS change of shape with a significant shear component, in the transformed region* [Bilby and Christian, 1956]. Table 1.1 shows a comparison of the characteristics of all the three types of transformations.

Table 1.1: *Comparison of reconstructive, displacive and martensitic transformations (adapted from Bhadeshia, [1987a]).*

| Characteristic/Feature | Transformation Product | | |
| --- | --- | --- | --- |
| | Reconstructive | Martensitic | Displacive |
| Diffusion of substitutional alloying elements | yes | no | no |
| Diffusion of interstitial alloying elements | yes | no | no |
| Atomic correspondence between the parent and product phases | nil | yes | yes |
| Movement of atoms | random | coordinated | coordinated |
| Morphology | not particular | plate or lath | plate or lath |
| IPS shape change | nil | yes | yes |
| Composition of the product phase | equilibrium or paraequilibrium | same as parent phase | equilibrium or paraequilibrium |
| Rational orientation with parent austenite | no | yes | yes |
| Can cross prior austenite grain boundaries? | yes | no | no |

## 1.3 Interface Structures

The $\gamma \rightarrow \alpha$ transformation is a first order transformation§, which occurs by the

§ In second order transformations the parent and product phases do not coexist and there is no identifiable interface. The transformation happens in all regions of the parent phase.

motion of well defined interfaces. The structure of the interfaces influences the way in which the atoms of the parent lattice move in order to generate the $\alpha$ lattice. The interfaces may be divided into fully coherent, semi coherent, and incoherent interfaces [Chadwick, 1972; Bruke, 1965].

### 1.3.1 *Fully Coherent Interfaces*

A fully coherent interface arises when the two crystals match perfectly at the interface plane, so that the two lattices are continuous across the interface (Fig. 1.2a). This can only be achieved if, disregarding chemical species, the interfacial plane has same atomic configuration in both phases i.e., rows and planes of atoms are continuous across this interface and this requires the two crystals to be orientated relative to each other in a special way. A twin boundary in a single phase material is an example of a perfectly coherent boundary.

When the distance between the atoms in the interface is not identical it is still possible to maintain coherency by straining one or both of the two lattices as illustrated in Fig. 1.2b. The resultant lattice distortions are known as coherency strains. If these strains are not too large they can be accommodated by dilatation in the plane of the interface.

In the situation when the two lattices match perfectly at the interface, the surface energy between precipitate and lattice is virtually nil, making the nucleation barrier small. However, if the equilibrium (stress free) lattice parameters of the solute-rich phase and the matrix differ, the precipitate will be strained so that the $E^{str}$ is always positive.

The coherent interfaces imply a definite orientation relationship between the precipitate lattice and the matrix.

### 1.3.2 *Semi-Coherent Interface*

A semi-coherent interface may be regarded as an interface in which regions of coherency are separated by regions of discontinuity (Fig. 1.2b). The structures do not really fit at the interface, and the mismatch would accumulate unless periodically corrected. There are two kinds of semi-coherency [Christian, 1975b]: i) glissile interfaces and ii) epitaxial semi-coherency.

### *1.3.2.1 Glissile Interfaces*

If the discontinuities discussed above consist of a single set of screw dislocations *i.e.,* when the transformation strain is an invariant-line strain (consisting of the Bain strain and an appropriate rigid body rotation), and the invariant-line lies in

the interface [Christian, 1969], then the latter need only contain a single set of misfit dislocations. For martensitic transformations, the transformation strain has to be an invariant-line strain in order to ensure a glissile interface [Christian, 1969]. A glissile interface also requires that the glide planes (of the misfit dislocations) associated with the $\alpha$ lattice meet the corresponding glide planes in the $\gamma$ lattice edge to edge in the interface, along the dislocation lines.
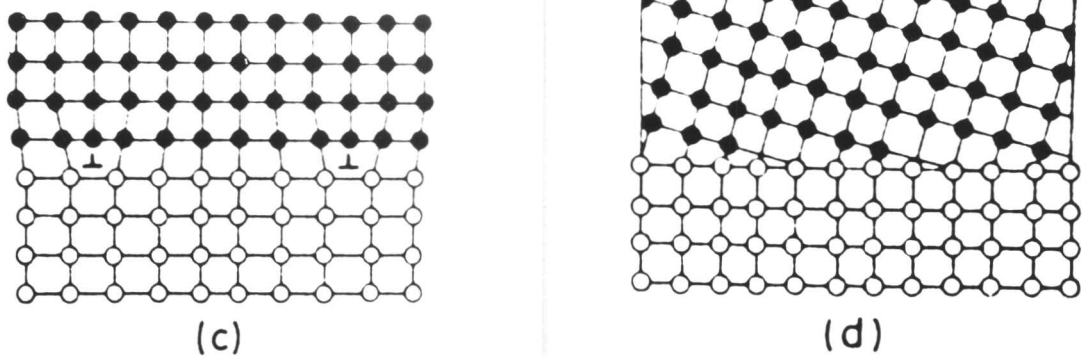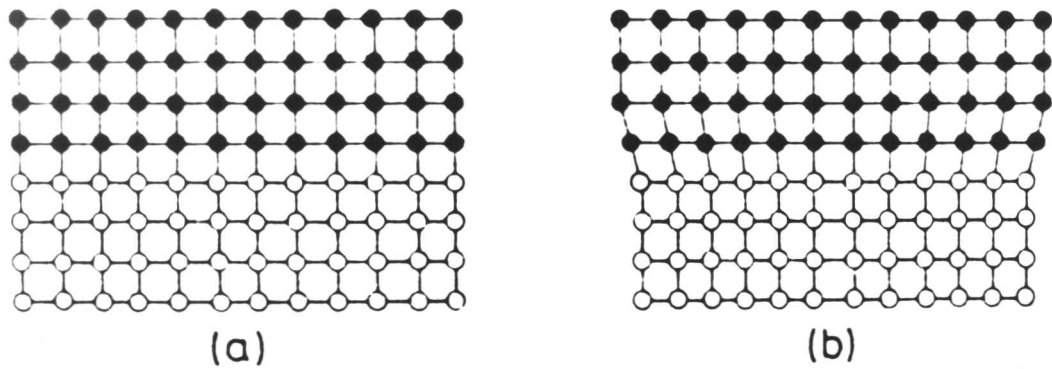


Fig. 1.2: *Schematic drawings of the atomic arrangements at interfaces [Chadwick, 1972]. a) Perfectly coherent. b) Elastically strained coherent. c) Semi-coherent. d) Incoherent.*

Glissile $\alpha/\gamma$ interfaces can move conservatively and when they do so, the interface dislocations homogeneously shear the volume of material swept by the interface in such a way that the macroscopic shape change accompanying the transformation is an IPS, even though the homogeneous lattice transformation strain is an invariant-line strain. Conservative motion of a glissile interface leads to martensitic transformation.

### 1.3.2.2 Epitaxial Semi-Coherency

If the intrinsic interface dislocations have Burger's vectors which lie in the interface plane, not parallel to the dislocation line, then the interface is said to be "epitaxially semi-coherent" (Fig. 1.3). The normal displacement of such an interface necessitates the thermally activated climb of the misfit dislocations, so that the interface can only move in a non-conservative manner with relatively restricted mobility at low temperatures.
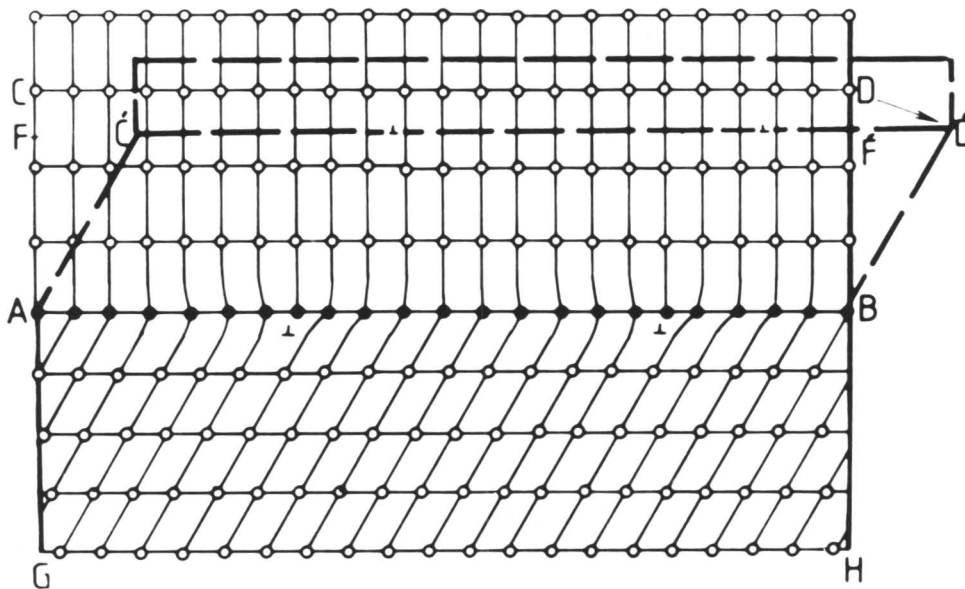


Fig. 1.3: *Diagrammatic illustration of the shape change accompanying the movement of epitaxially semi-coherent interface [Bhadeshia, 1987b].*

The nature of the shape change that accompanies the motion of an epitaxially semi-coherent interface is difficult to assess. As discussed by Christian [1975b, 1969], the upward non-conservative motion of the boundary AB (Fig. 1.3) to a new position CD' should change the shape of a region ACDB of the parent crystal to a shape AC' D' B of the product phase. The shape change thus amounts to a uniaxial distortion normal to AB together with a shear component parallel to the interface plane (i.e. an IPS). Because of the dislocations climb in the process, the total number of atoms in the regions ACDB and AC' D' B will not be equal, the difference being removed by diffusion normal to the interface plane. Atomic movements are therefore necessary over a distance (at least) equal to that moved by the boundary, corresponding to the thickness of the transformed region. If this constitutes the only reconstructive flux that accompanies interface motion, then the shear component of the shape change will not be destroyed, and the transformation will exhibit surface relief effects, normally associated with displacive transformations. The mobility will, of course, be limited by the climb process. A situation like this in effect amounts to an orderly diffusion of atoms as the interface migrates (i.e. removal of the extra half-planes of the misfit dislocations) so that a partial atomic correspondence is still maintained between parent and the product phases.

### 1.3.3 Incoherent Interfaces

As the misfit between adjacent crystals increases, the dislocations in the connecting interface become more closely spaced. They eventually coalesce so that the boundary consists of closely spaced "vacancies" or "dislocation cores". Such a boundary is said to be incoherent; there is a little correlation of atomic positions across the boundary.

In general, incoherent interfaces result when two randomly orientated crystals are joined across any interfacial plane as shown in Fig. 1.2d. They may, however, also exist between crystals with an orientation relationship if the interface has a different structure in the two crystals. They are characterised by a high energy ($\simeq$ 0.5-1.0 J m$^{-2}$) [Porter and Easterling, 1988], insensitive to the orientation of the interfacial plane.

### 1.3.4 Interface Mobility

During a phase transformation, one crystal grows at the expense of the other by the migration of the boundary interface. It is clear that if the structures are fully coherent a lattice correspondence is implicit in this process, so that labelled rows or planes of lattice sites in one crystal become rows or planes in the other.

The motion of a coherent boundary without diffusion thus produces a macroscopic change of shape which is specified by the relation between the lattices.

In a semi-coherent boundary, since the lattice deformations are not compatible, the motion of the boundary cannot produce a change of shape given by the local atomic correspondence. The shape change produced is obtained by combining the lattice change with the change due to the migration of the discontinuities in the boundary (lattice-invariant deformation). It follows that for both fully coherent and semi-coherent boundaries the shape change produced by motion of the boundary is an invariant-plane strain [Christian, 1975b].

If the boundary is incoherent, there is no correspondence between parent and the product phases and no shape change when it moves. The motion of an incoherent boundary can only cause reconstructive transformations. Thus the growth of a mechanical twin changes the shape of the specimen, but the motion of a general grain boundary or of an annealing twin does not.

Incoherent, coherent and semi-coherent boundaries can coexist around a particle which has grown diffusionally by reconstructive transformation. Only semi-coherent and coherent boundaries can exist around a particle which has grown displacively.

## 1.4 Shape Change Due to Martensitic Transformations

The salient feature of a martensitic transformation is that the transformed region undergoes a change of shape, if a surface of the parent crystal is polished to be flat before the transformation. The nature of the shape deformation in the transformed region has been discussed by Bilby and Christian [1956], and is shown schematically in Fig. 1.4, where a martensite plate LMNOABCD meets a plane surface EFGH. In the region of the plate, the surface is tilted about the lines AB and CD. The surface ABCD remains plane, and a scratch SS' remains continuous and deforms into straight sections STT' S'.

The shape deformation thus deforms planes into planes and straight lines into straight lines; such a deformation is called "homogeneous". It is evident that if cavities are not to appear along the surfaces ABML and DCNO, there can be no rotation of these surfaces as the plate thickens. The experimental observation that the plate and matrix may be kept in focus with a high-powered objective throughout their length shows further that the lines AB cannot be rotated by more than a few minutes of arc. Since the free surface EFGH is arbitrary, it follows that no line
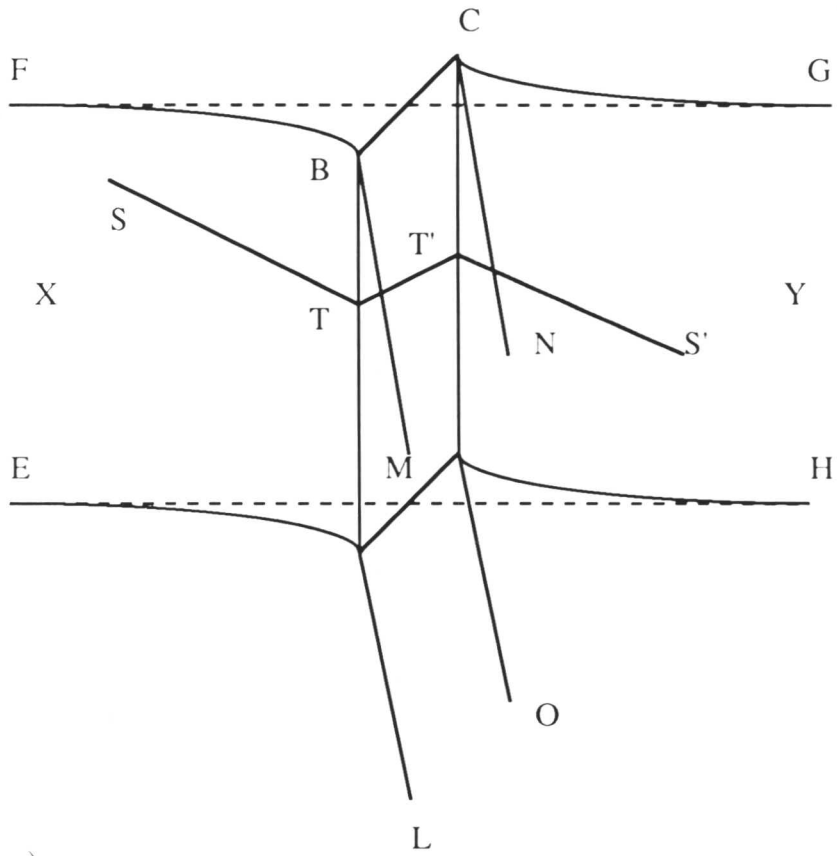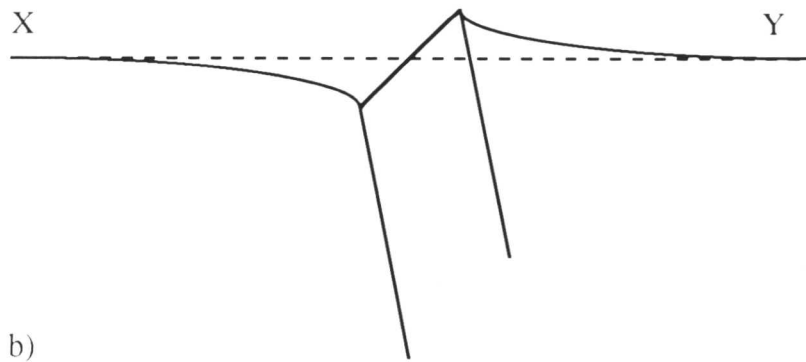
Fig. 1.4: *a) The shape change associated with a martensite plate. b) Section through XY [Bilby and Christian, 1956].*

in the interface ABML (or DCNO) is rotated. It remains possible that there is a contraction or expansion uniform in all directions of these surfaces (a negative or positive dilatation), since this would leave all lines in the surfaces unrotated.

A section through XY shown in Fig. 1.4b, illustrates that there is considerable elastic distortion induced in the matrix around the plate due to the preservation of continuity at the interface. This distortion imposes constraints on the growing crystal and causes it to adopt the form of a lenticular plate, the usual form of martensite crystals.

## 1.5 Invariant-Plane Strain

If the operation of a strain, leaves one plane of the parent crystal completely unrotated and undistorted; this is known as an invariant-plane strain (IPS). Fig. 1.5, illustrates three such strains. Fig. 1.5a is an example of invariant-plane strain which is purely dilatational, and is of the type to be expected when a plate-shaped precipitate grows reconstructively. This type of IPS reflects the volume changes accompanying the transformation. In Fig. 1.5b, the invariant-plane corresponds to a simple shear, involving no change of volume, as homogeneous deformation of crystal by slip. The shape of the parent crystal alters in a way which reflects the shear character of the deformation. The most general invariant-plane strain (Fig. 1.5c) involves both a volume change and a shear and associated with the martensitic transformations.



Uniaxial extension
(a)

Simple shear
(b)

General IPS
(c)
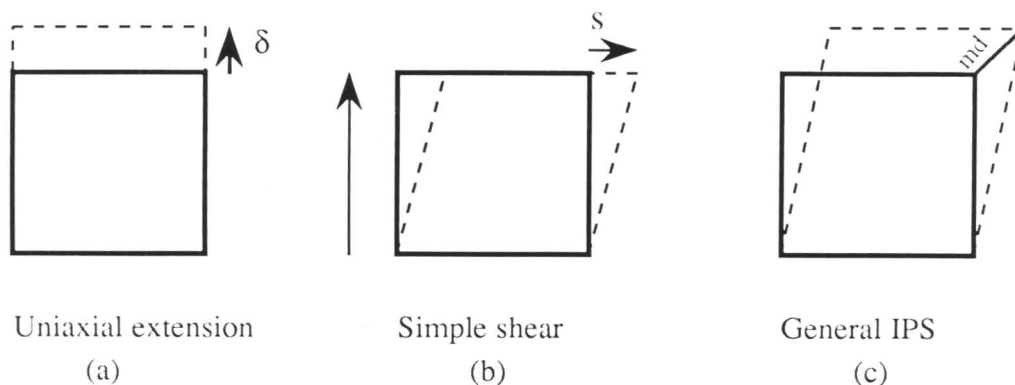
Fig. 1.5: *Three kinds of invariant-plane strains. The heavy lines indicate the shape before deformation, s, δ and md respectively [Bhadeshia, 1987b].*

## 1.6 The Effects of Alloying Elements

The addition of alloying elements to steels affects both the thermodynamics and kinetics of the decomposition of austenite. The aim of this section is to mention briefly how alloying additions influence the transformations. Alloying elements in steel can be classified as substitutional, slow diffusers requiring vacant lattice sites, and interstitial, fast diffusers which occupy the sublattice of interstices, and either or both can control growth rate depending on the driving force. If the local equilibrium is maintained at the $\alpha/\gamma$ interface, two modes of proeutectoid ferrite growth in an Fe-C-X system (where X is a substitutional alloying element) are possible, depending on alloy composition. These modes are characterized as follows [Coates, 1973]:

### 1.6.1 *Partition-Local Equilibrium (P-LE)*

For low supersaturations, X partitions between the ferrite ($\alpha$ ) and parent austenite ($\gamma$ ) phase. The flux of carbon is reduced by making the C-concentration gradient very shallow. The precipitate growth rate is low and is determined by the slow diffuser, X, i.e., X exerts a reconstructive drag on the growth kinetics, which is a consequence of the fact that it diffuses many orders of magnitude slower than carbon. Fig. 1.6, shows ferrite growth occurring with local equilibrium at the $\alpha/\gamma$ interface in Fe-Mn system.

### 1.6.2 *Negligible Partition-Local Equilibrium (NP-LE)*

For higher supersaturations, the precipitate growth rate is relatively high and is determined by the fast diffuser, C. In this regime, X, exerts essentially no reconstructive drag effect, in spite of its low diffusivity. The gradient of X is made very steep to increase the flux, by partitioning very little X between $\gamma$ and $\alpha$. A given bulk composition is expected to pass from NP-LE to P-LE regime with increasing temperature. During NP-LE growth, the width of the X concentration spike in $\gamma$ is a few nanometers. As the temperature of transformation decreases the X concentration spike also decreases until it becomes approximately equal to atomic dimensions. The condition is then reached where the substitutional atoms become configurationally frozen, and equilibrium breaks down at the interface. This constrained equilibrium, in which X is not redistributed during transformation is known as "Para-equilibrium". However, C is still mobile, and subject to the constraint that Fe/Mn ratio is identical in $\alpha$ and $\gamma$, it reaches equilibrium.
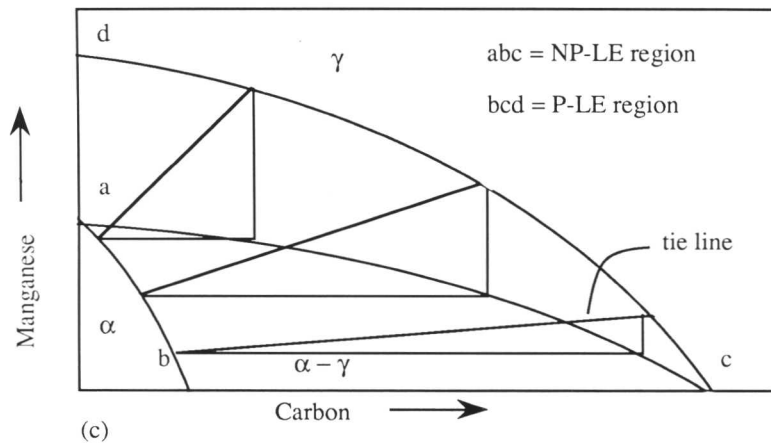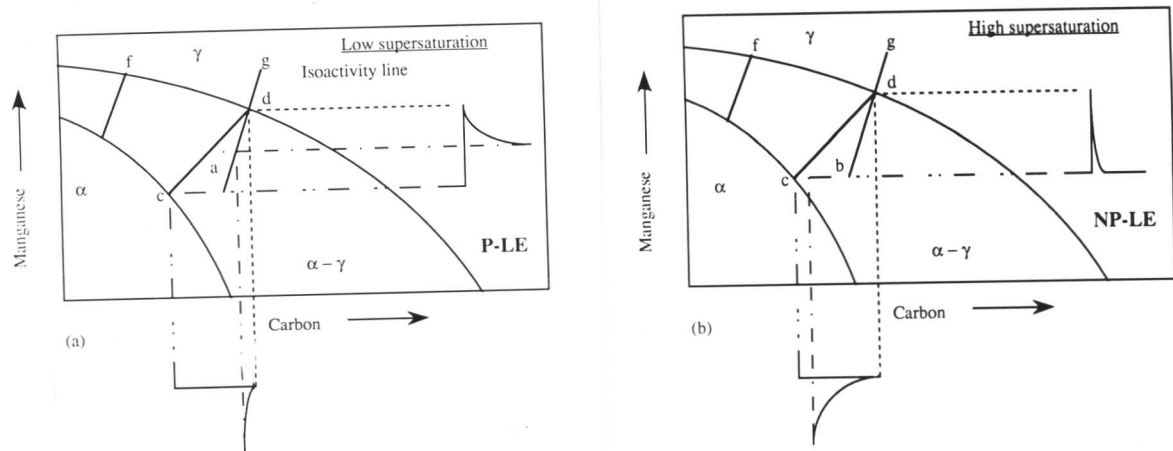
Fig. 1.6: *Schematic isothermal sections of the Fe-Mn-C system, illustrating ferrite growth occurring with local equilibrium at the α/γ interface [Bhadeshia, 1985a]. (a) Growth at low supersaturations (P-LE) with bulk redistribution of Mn. (b) Growth at high supersaturations (NP-LE) with negligible partitioning of Mn during transformation. The bulk alloy compositions are designated "A" and "B" in (a) and (b) respectively. c) Division of α + γ phase field into domains where either the P-LE or NP-LE mechanisms can operate.*

## 1.7 Classification of Ferritic Microstructures

The decomposition of the higher temperature face-centered cubic $\gamma$ -iron to the less dense body-centered cubic allotrope ($\alpha$ ) gives rise to a variety of different morphologies and microstructures depending upon the cooling rate, presence of alloying elements, the availability of lower energy nucleation sites for heterogeneous nucleation. Thus austenite can decompose into allotriomorphic ferrite, Widmanstätten ferrite, acicular ferrite, bainite, pearlite and martensite. A classification scheme for the products formed by the decomposition of austenite based on the nucleation and growth mechanism is presented in Fig. 1.7.
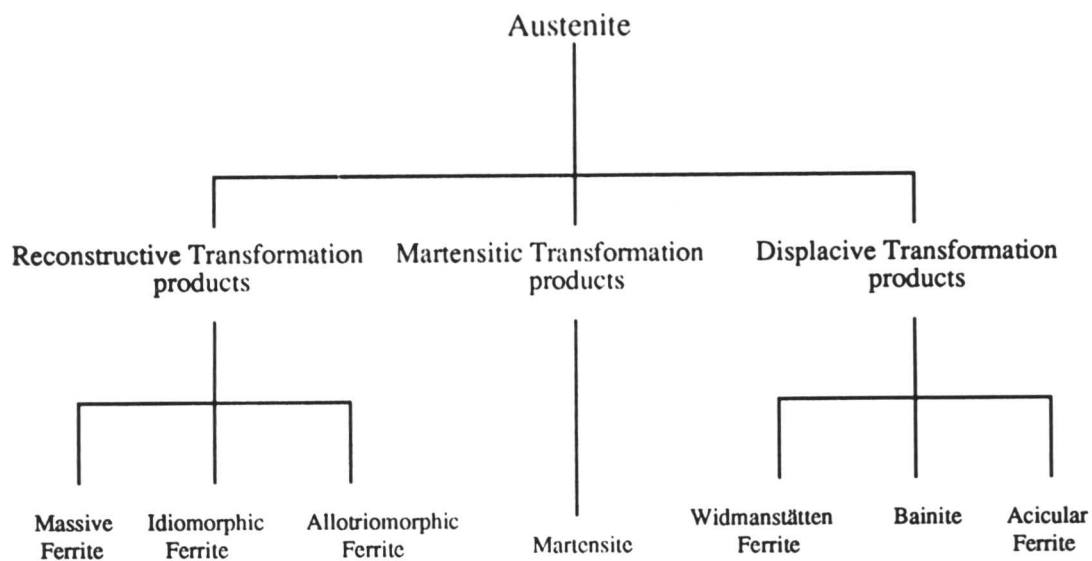


Fig. 1.7: *Classification of transformation products formed by decomposition of austenite according to the nucleation and growth mechanisms.*

## 1.8 Reconstructive Decomposition of Austenite

Ferrite which grows by a reconstructive transformation mechanism can be classified into two main forms: allotriomorphic ferrite and idiomorphic ferrite.

### 1.8.1 *Allotriomorphic Ferrite*

The term "allotriomorphic" means that the phase is crystalline in internal structure but not in outward form. It implies that the limiting surfaces of the crystal are not regular and do not display the symmetry of its internal structure [Bhadeshia, 1985]. The allotriomorphic ferrite (Fig. 1.8a) which nucleates at prior austenite grain boundaries tends to grow along the $\gamma$ -grain boundaries at a rate faster than in the direction normal to plane, so that its shape is influenced strongly by the presence of the boundary and hence does not necessarily reflect its internal symmetry. Of course, allotriomorphic ferrite need not form just at austenite grain boundaries; but it invariably does so, presumably because there are no other suitable (two-dimensional) heterogeneous nucleation sites in austenite.

The allotriomorphic ferrite grains nucleate at the highest temperatures, i.e. just below $Ae_3$, and during the growth stage have a semi-coherent interface with the other adjacent abutting grain. As the transformation temperature is lowered, these crystals develop facets on at least one side of the boundary (Fig. 1.8).

### 1.8.1.3 *Growth of Allotriomorphic Ferrite*

The kinetics of allotriomorphic ferrite reaction play an important role in determining the hardenability of steels and also is very important to microstructural predictions as this determines the volume fraction of austenite available to transform into the other phases and the carbon enrichment of the remaining austenite has occurred. A high volume fraction of allotriomorphic ferrite would necessarily limit the amount of austenite left for further different decomposition reactions to follow. Hence any errors in the volume fraction of allotriomorphic ferrite ($V_\alpha$) will be magnified throughout the rest of the factors controlling $V_\alpha$, as the large volume fraction is associated with poor toughness [Levine and Hill, 1977]. The large width of allotriomorphic ferrite allows cracks to develop a large size so that at low temperatures propagation of such defects occurs readily.

The growth of allotriomorphic ferrite $\alpha$ can be treated in terms of the normal migration of planar $\gamma/\alpha$ interfaces. It is noted that the growth of $\alpha$ in dilute steels occurs without the bulk partitioning of substitutional alloying elements [Aaronson and Domain, 1966], especially when the growth rates involved are large [Coates,
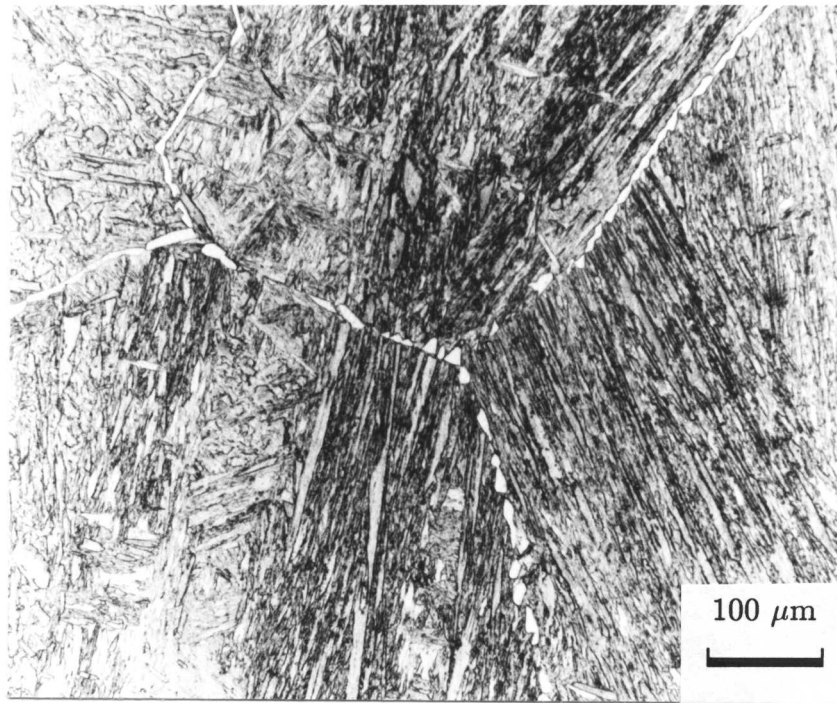
(a)
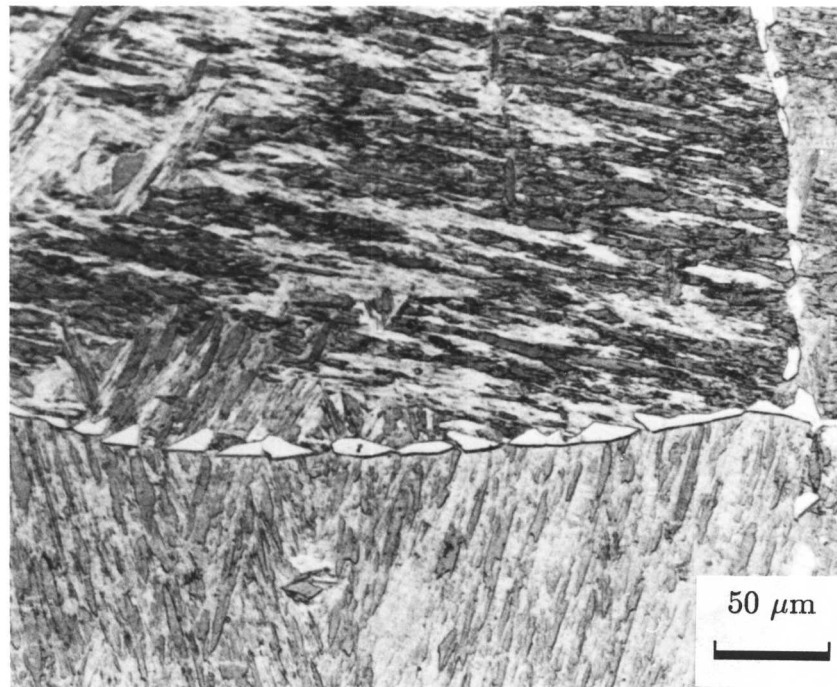


(b)

Fig. 1.8: *Optical micrographs showing heterogeneous nucleation of allotriomorphic ferrite at prior austenite grain boundaries and they subsequently grew along these boundaries and growth of allotriomorphic ferrite at prior austenite grain boundaries in Fe-0.22C-2.05Si-3.07Mn-0.7Mo (wt. %) steel austenitised at 1100 °C for 10 min and transformed at (a) 750 °C @ 20 hr (b) 735 °C@ 20 hr.*

1973; Glimour *et al.* 1972], as is the case for weld deposits. In these circumstances, ferrite growth can occur at a rate controlled by diffusion of carbon in the austenite ahead of the interface. If it is assumed that the growth of the layer of $\alpha$ is diffusion-controlled (diffusion of carbon) in austenite, and that for alloy steels the transformation occurs under paraequilibrium conditions [Bhadeshia, 1985], then for isothermal transformation the volume fraction of allotriomorphic ferrite should depend mainly on the parabolic rate constant $\alpha_1$,

$$q = \alpha_1 t^{0.5} \tag{1.1}$$

where $q$ is the half-thickness of the allotriomorphic ferrite layer and $t$ is the time, defined to be zero when $q=0$. The numerical value of $\alpha_1$ can obtained by solving the equation [Christian, 1975b],

$$\frac{2(x^{\gamma\alpha} - \overline{x})}{(x^{\gamma\alpha} - x^{\alpha\gamma})}(\frac{\overline{D}}{\pi}) = \alpha_1 [exp(\frac{\alpha_1^2}{4D})][1 - erf(\frac{\alpha_1}{\sqrt{2\overline{D}^{1/2}}})] \tag{1.2}$$

where $x^{\gamma\alpha}$ is the paraequilibrium carbon content in the austenite, $x^{\alpha\gamma}$ is the paraequilibrium carbon content in the ferrite, $\overline{x}$ is the average carbon concentration of the alloy and $\overline{D}$ is the weighted average diffusivity of carbon in the austenite [Bhadeshia, 1981b].

### 1.8.2 *Idiomorphic Ferrite*

The term idiomorphic implies that the phase concerned has faces belonging to its crystalline form. In steels, idiomorphic ferrite is taken to be that which has a roughly equiaxed morphology (Fig. 1.9). Idiomorphic ferrite usually forms intragranularly [Bhadeshia, 1985], presumably at inclusions or other heterogeneous nucleation sites.

Since both idiomorphic and allotriomorphic ferrite grow by a reconstructive transformation mechanism, their growth is not restricted by austenite boundaries. The extent of penetration into particular grains may vary since interface mobility can change with $\alpha/\gamma$ orientation relationship.

### 1.8.3 *Massive Ferrite*

Massive ferrite, which also grows by a reconstructive transformation mechanism, has the distinction that it inherits the composition of the parent austenite. The ability to cross parent austenite grain boundaries seems particularly pronounced during massive transformation; the final ferrite grain size can be larger than the initial grain size of the austenite. The lack of composition change allows
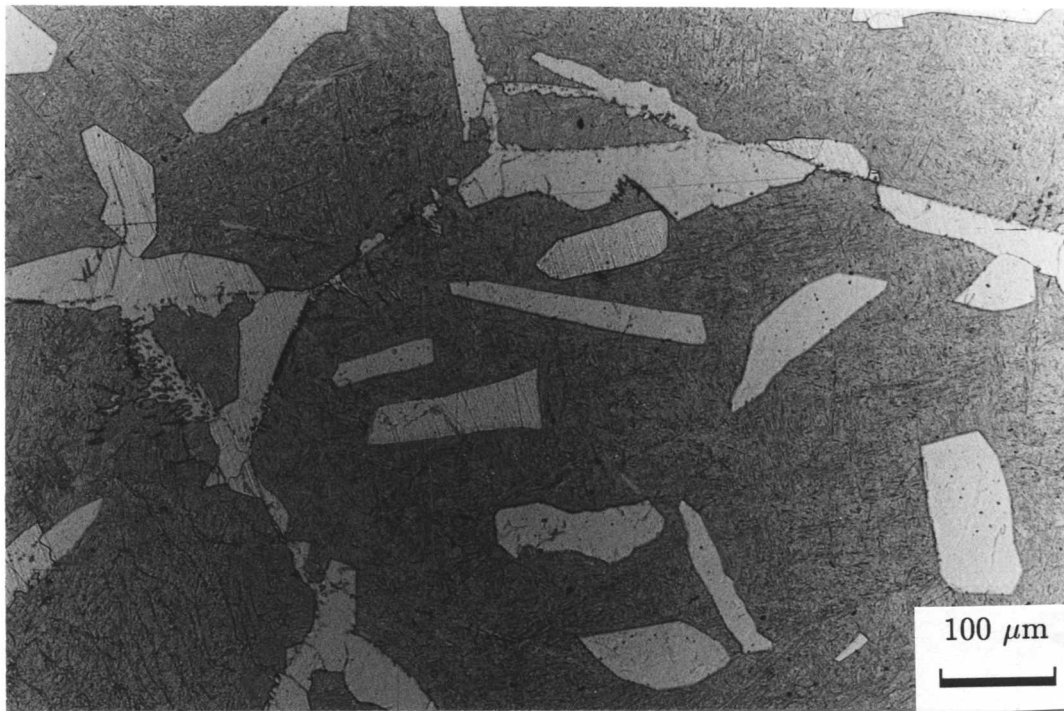
Fig. 1.9: *Formation of idiomorphic ferrite in alloy Fe-0.39C-2.05Si-4.08Ni (wt. %) steel, austenitised at 1300 °C @ 30 min and transformed at 680 °C @ 3hr.*
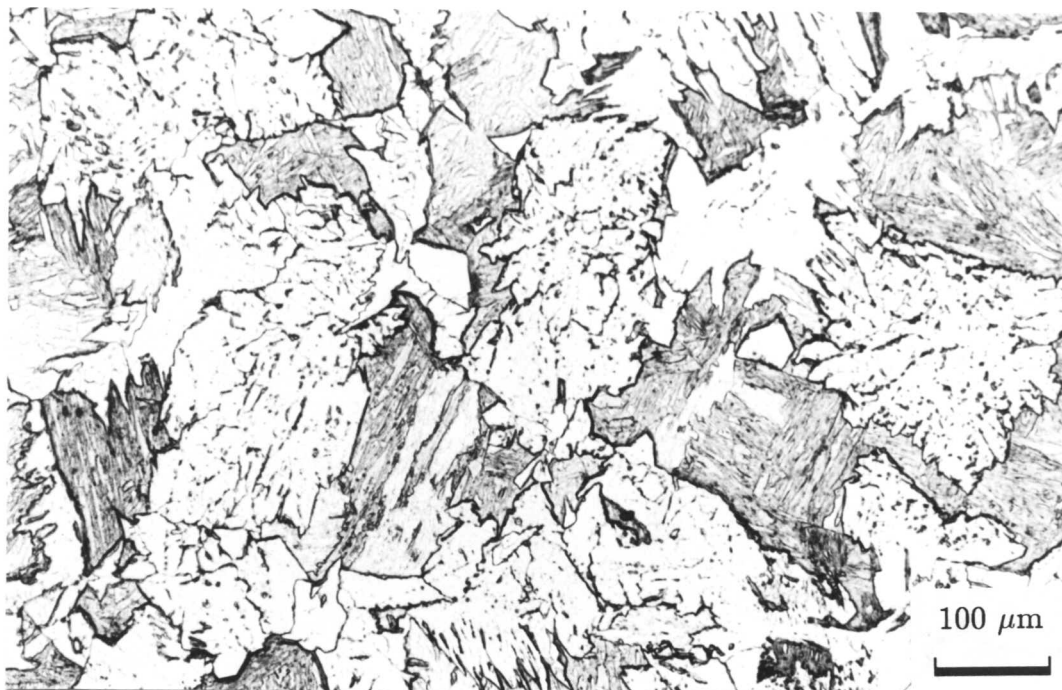


Fig. 1.10: *Formation of massive ferrite in alloy Fe-0.05C-2.05Si-4.08Ni (wt. %) steel, austenitised at 1300 °C @ 10 min and transformed at 600 °C @ 60 s.*

the transformation to proceed until all of the austenite is consumed. These factors combined to give a single-phase microstructure of larger grains of ferrite which have an approximately equiaxed morphology due to impingement between neighbouring grains as shown in the micrograph of Fig. 1.10.

## 1.9 Displacive Decomposition of Austenite

The products resulting from displacive decomposition of austenite can be, Widmanstätten ferrite, bainite, acicular ferrite and martensite, depending upon chemical composition and transformation temperature. The displacive transformation products are very important form engineering point of view, because the volume fraction of these products directly affects the mechanical properties of the steels. For example steels in bainite conditions show a remarkable combination of strength and toughness [Nakasugi *et al.* 1983] and the large volume fraction of acicular ferrite enhances the toughness [Garland and Kirkwood, 1975].

### 1.9.1 *Widmanstätten Ferrite*

Widmanstätten ferrite is a phase formed by the transformation of austenite below $Ae_3$. It forms in a temperature range where reconstructive transformations become relatively sluggish and give way to displacive transformations. Widmanstätten ferrite which grows by a displacive transformation mechanism, maintains an atomic correspondence between the parent and product phases. On an optical scale, Widmanstätten ferrite has the shape of a thin wedge (Fig. 1.11), the actual shape being somewhere between that of a plate and a lath§.

Widmanstätten ferrite can nucleate either directly from austenite grain boundaries, called "Widmanstätten ferrite primary side plates" or it can nucleate from previously formed grain boundary allotriomorphic ferrite, "Widmanstätten ferrite secondary side plates", both morphologies are shown in Fig. 1.12.

Widmanstätten ferrite ($\alpha_W$) formation generally involves the cooperative growth of two mutually accommodating plates. The adjacent plates generally turn out to be similarly oriented, presumably because the simultaneous nucleation of such variants is relatively easy [Bhadeshia, 1981a]. Widmanstätten ferrite forms at low undercoolings below the $Ae_3$ temperatures, where the driving force for the transformation is small, with an equilibrium or paraequilibrium carbon content.

---

§ If a plate or lath is idealized as a rectangular parallelepiped with sides of lengths, a, b, and c then $a = b >> c$ for plate and $a >> b >> c$ for lath [Bhadeshia, 1985].
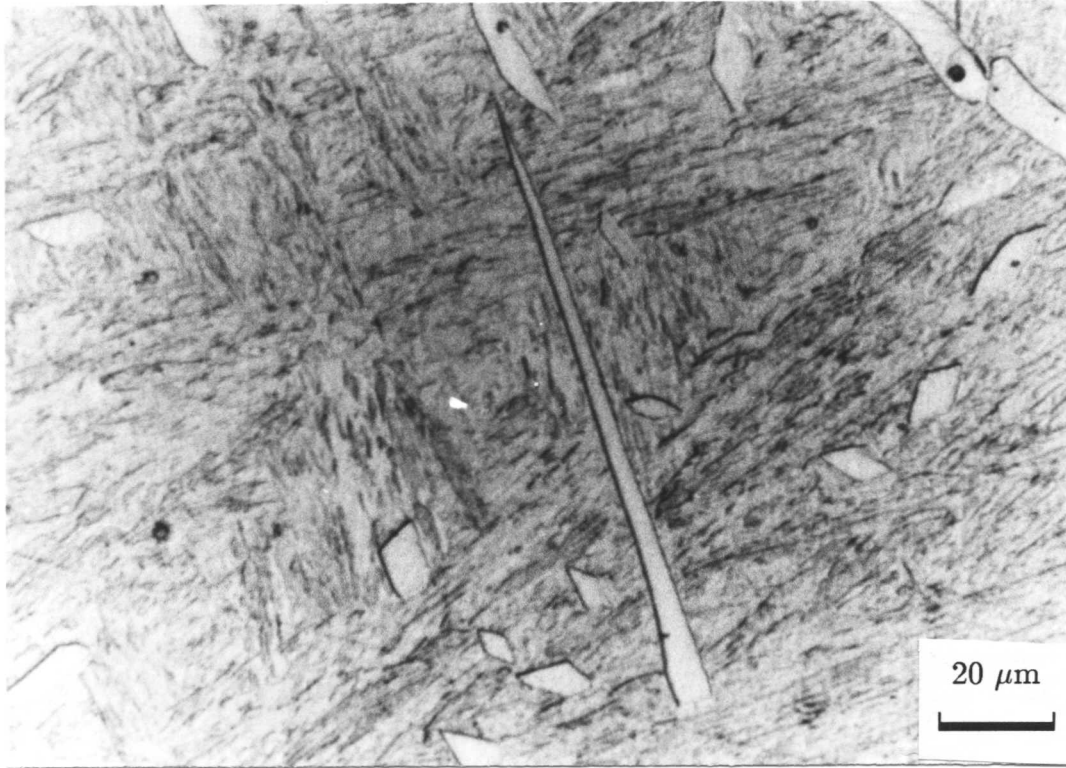
Fig. 1.11: *Optical micrograph showing the classical wedge shape of Widmanstätten ferrite in Fe-0.22C-2.05Si-3.07Mn-0.7Mo (wt. %) steel transformed at 700 °C @ 25 days after austenitisation at 1100 °C @ 10 min.*

Since the partitioning of carbon at these temperature is a thermodynamic necessity and since the transformation interface is glissile, the growth of Widmanstätten ferrite is controlled by the diffusion of carbon in the austenite ahead of the interface.

The formation of Widmanstätten ferrite is also accompanied by a change in the shape of the transformed region [Bhadeshia, 1981a; Watson and McDougall, 1973]. The shape change due to a single wedge of Widmanstätten ferrite consists of two adjacent and opposing invariant-plane strain (IPS) deformations [Bhadeshia, 1981a]. These IPS deformations each have a large shear component (0.4) [Watson and McDougall, 1973] and imply the existence of an atomic correspondence between the parent and product phases as far as the iron and substitutional solute atoms are concerned. Interstitial atoms like carbon can diffuse during growth without affecting the shape change or the displacive character of the transformation [Bhadeshia, 1985]. The cooperative growth of a pair of adjacent mutually-accommodating crystallographic variants allows the elastically accommodated strain energy

(a)



(b)
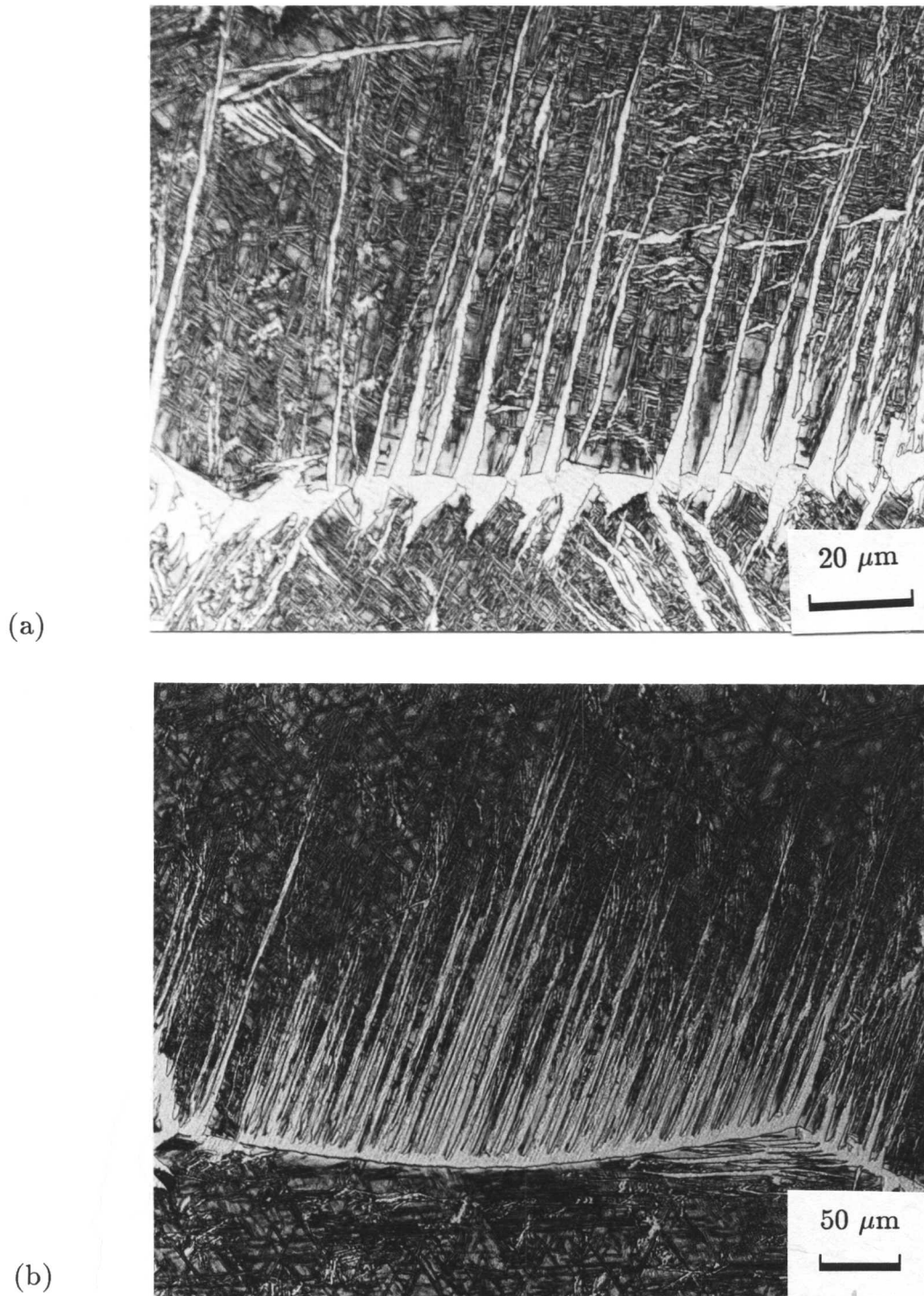
Fig. 1.12: *Optical micrographs showing various forms of Widmanstätten ferrite in a Fe-0.42C-2.0Si (wt. %) steel. (a) Primary Widmanstätten ferrite formed directly from the prior austenite grain boundaries (1300 °C @ 30 min→ 680 °C @ 60 s). (b) Secondary Widmanstätten ferrite formed from the allotriomorphic ferrite (1300 °C @ 10 min + 680 °C @ 5 min).*

accompanying plate formation to be rather small, of the order of 50 J mol$^{-1}$ [Bhadeshia, 1981a]. This is consistent with the low undercoolings at which Widmanstätten ferrite forms and the wedge morphology which arises because the adjacent variants have slightly different habit planes. The shape change indicates that the $\alpha/\gamma$ interface is glissile and the plates therefore grow at a constant rate controlled by the diffusion of carbon in the austenite ahead of the plate tip. Widmanstätten ferrite cannot be put into the group of reconstructive transformation products, because there is no diffusion involved in the actual lattice change, iron and substitutional elements do not diffuse during transformation. There is no reconstructive diffusion during the formation of Widmanstätten ferrite.

### 1.9.2 *Bainite*

Bainite forms by the decomposition of austenite at a higher undercooling relative to Widmanstätten ferrite and grows in the form of sheaves originating from austenite grain boundaries. The sheaf consists of much smaller platelets (sub-units) of ferrite. The sheaf itself has a wedge shaped plate morphology on a macroscopic scale.

When carbon is present, cementite precipitation occurs from the austenite between the sub-units in the case of upper bainite; while in lower bainite, the cementite (or $\eta$-carbide) can also precipitate from within the bainitic ferrite.

### *1.9.2.4 Upper Bainite*

Upper bainite consists of platelets of ferrite adjacent to each other, which are in very nearly the same crystallographic orientation in space, so that whenever two adjacent plates touch, a low-angle boundary arises. Elongated cementite particles usually decorate the boundaries of these plates, the amount of these slabs of cementite depending on the carbon content of the steel. These ferrite platelets, which form a sheaf, have the same habit plane [Bhadeshia and Edmonds, 1979]. Sheaves of the upper bainite inevitably nucleate at prior austenite grain boundaries, and intragranular nucleation is not to be found.

The bainitic ferrite after transformation may retain a small supersaturation of carbon, and has a rational orientation relationship with the austenite. In silicon-containing steels, [Yang and Bhadeshia, 1987], it has been shown that sub-units within a sheaf of upper bainite can also be distinguished where no carbide forms but where the ferrite platelets are separated by films of carbon-enriched austenite (Fig. 1.13).

*1.9.2.5 Lower Bainite*

Lower bainite occurs at a lower temperature compared to upper bainite and is basically very similar to upper bainite, except that the amount of interplate cementite is less, and carbides can additionally be found within the ferrite plate itself. These intra-ferrite carbides can be $\eta$-carbides in the case of high carbon steels or cementite in the case of low carbon steels. It has been demonstrated [Yang and Bhadeshia, 1987] that $\eta$-carbides will not form in bainitic ferrite for steels with a carbon content below approximately 0.55 wt. %.

The carbide particles usually precipitate in a single crystallographic orientation such that their habit plane is inclined at about 60° to the plate axis. In some cases several variants have been observed [Bhadeshia and Edmonds, 1979], although the 60° variant still tends to dominate. The inter-plate carbide does not necessarily occur and results from the reconstructive decomposition of carbon-enriched austenite which has not transformed to ferrite. Lower bainite also forms as sheaves. A typical microstructure of lower bainite is shown in Fig. 1.14.

In both cases (upper bainite and lower bainite), the formation of a sub-unit is accompanied by an IPS shape change of the transformed region. Fig. 1.15 shows the surface relief accompanied by the formation of bainite. The sub-units within a given sheaf have the same habit plane, orientation relationship with the austenite, and shape deformation.

**1.9.3** *Acicular Ferrite*

Acicular ferrite which also grows by a displacive transformation mechanism [Yang and Bhadeshia, 1987] is not included in the Dubé [1948] classification. The morphology of acicular ferrite consists of non-parallel plates of ferrite within the austenite grains, (Fig. 1.16). During the early stages of the transformation, these plates nucleate on inclusions present in the austenite grains. The subsequent plates nucleate sympathetically on these inclusion-nucleated plates. Acicular ferrite is essentially, intragranularly nucleated bainite. The presence of acicular ferrite seems to be directly correlated with the improved toughness [Abson and Pargeter, 1986].
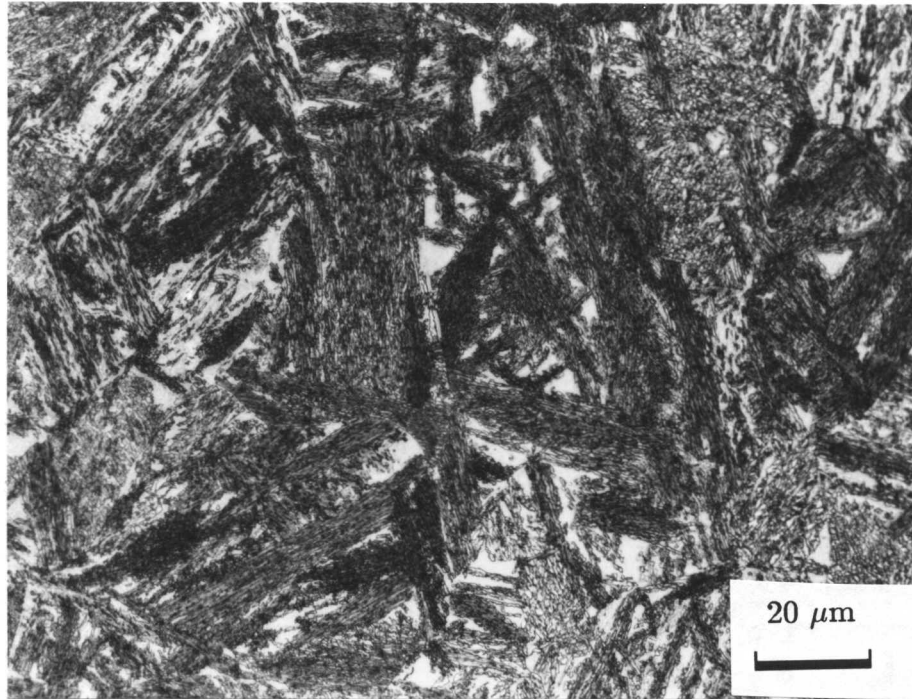
(a)
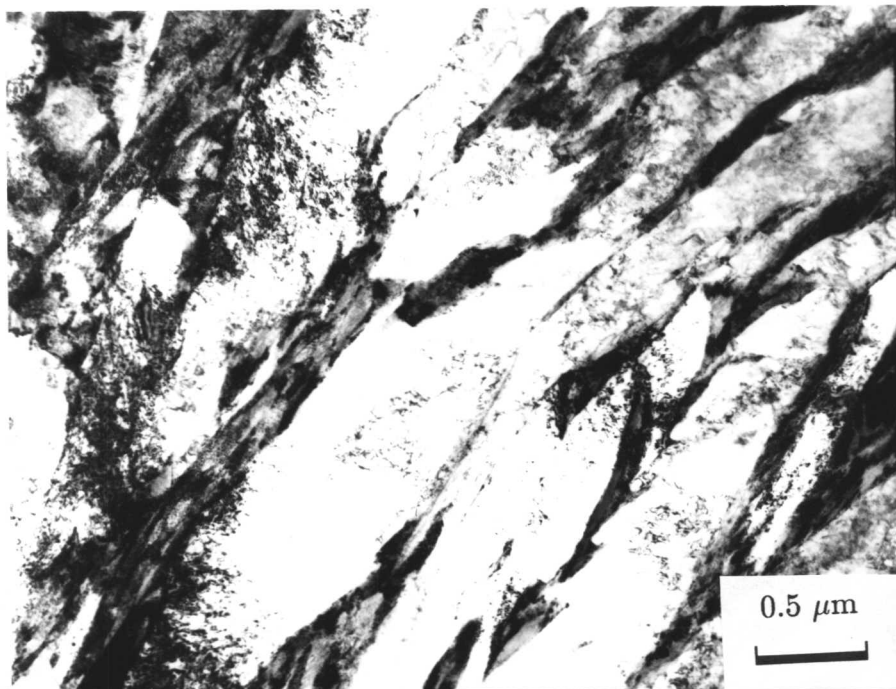


(b)

Fig. 1.13: *Micrographs showing bainite microstructure in Fe-0.22C-2.05Si-3.07Mn-0.7Mo (wt.%) alloy austenitised at 1000 °C @ 5 min and isothermally transformed at 400 °C @ 2000 s. (a) Optical micrograph. (b) Bright field TEM micrograph.*
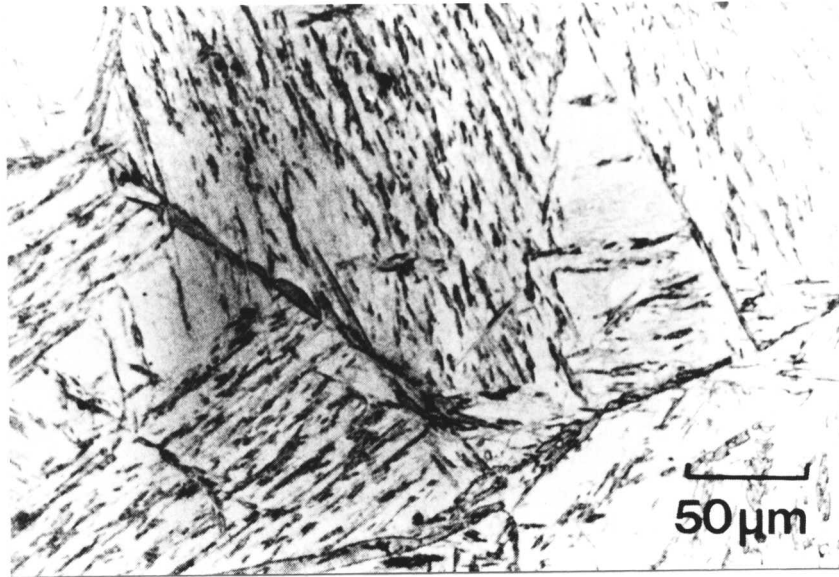
(a)
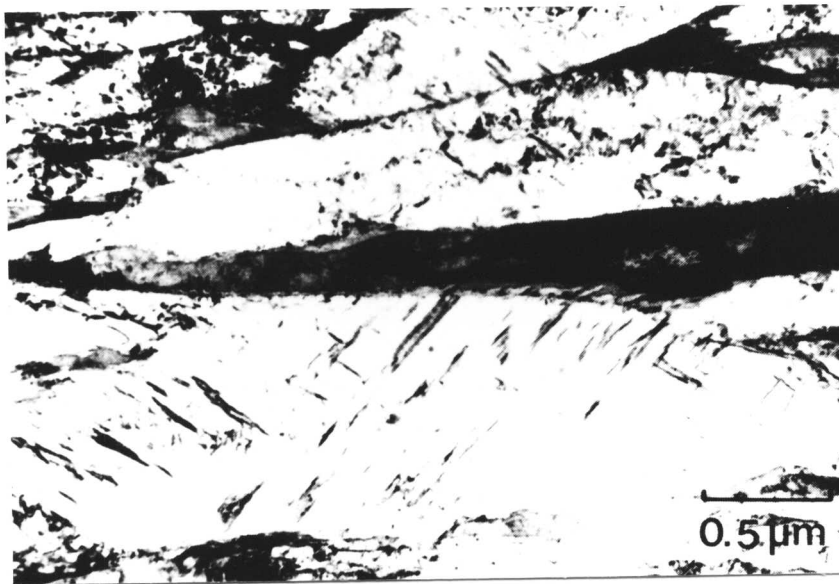


(b)

Fig. 1.14: *Micrographs showing lower bainite microstructure in Fe-0.43C-2.12Si-3.0Mn (wt.%) alloy austenitised at 1200 °C @ 5 min and isothermally transformed at 246 °C @ 30 min. (a) Optical micrograph. (b) Bright field TEM micrograph (after Bhadeshia and Edmonds, [1979]).*
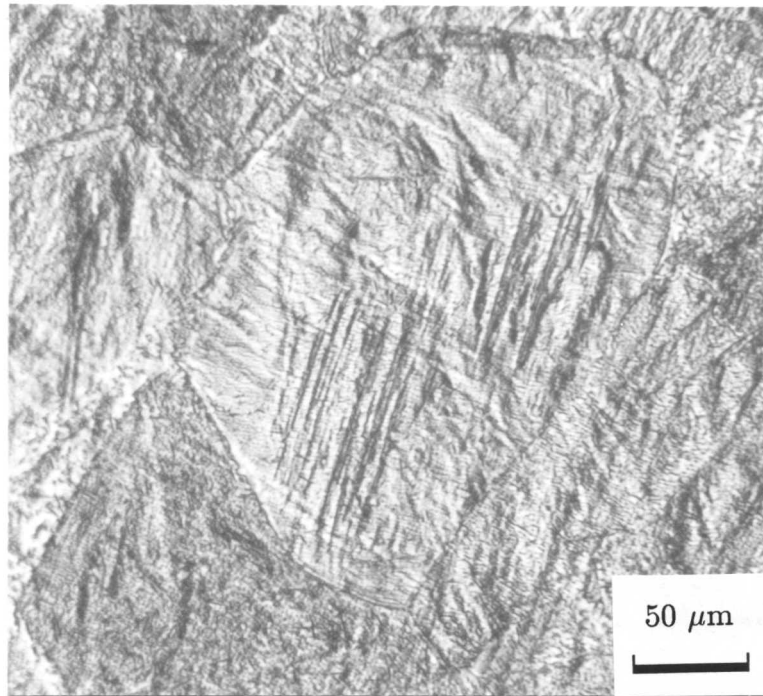
(a)
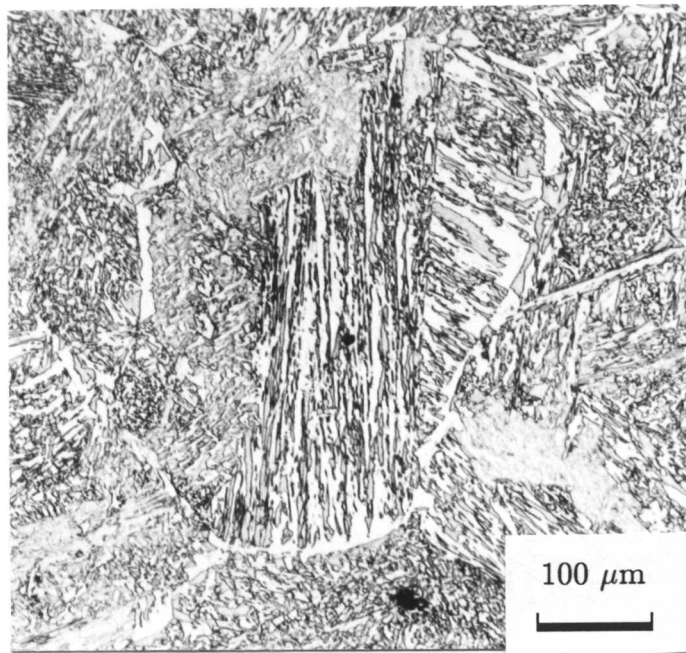


(b)

Fig. 1.15: *Micrographs showing the surface relief accompanied by the formation of bainite in Fe-0.22C-2.05Si-3.07Mn wt. % alloy. Specimen austenitised at 900 °C @ 5 min and isothermally transformed at 400 °C @ 1000 s. (a) Imaged by Nomarski interference contrast. (b) Same specimen after polishing on 6 μm diamond paste and etched.*

(a)



(b)
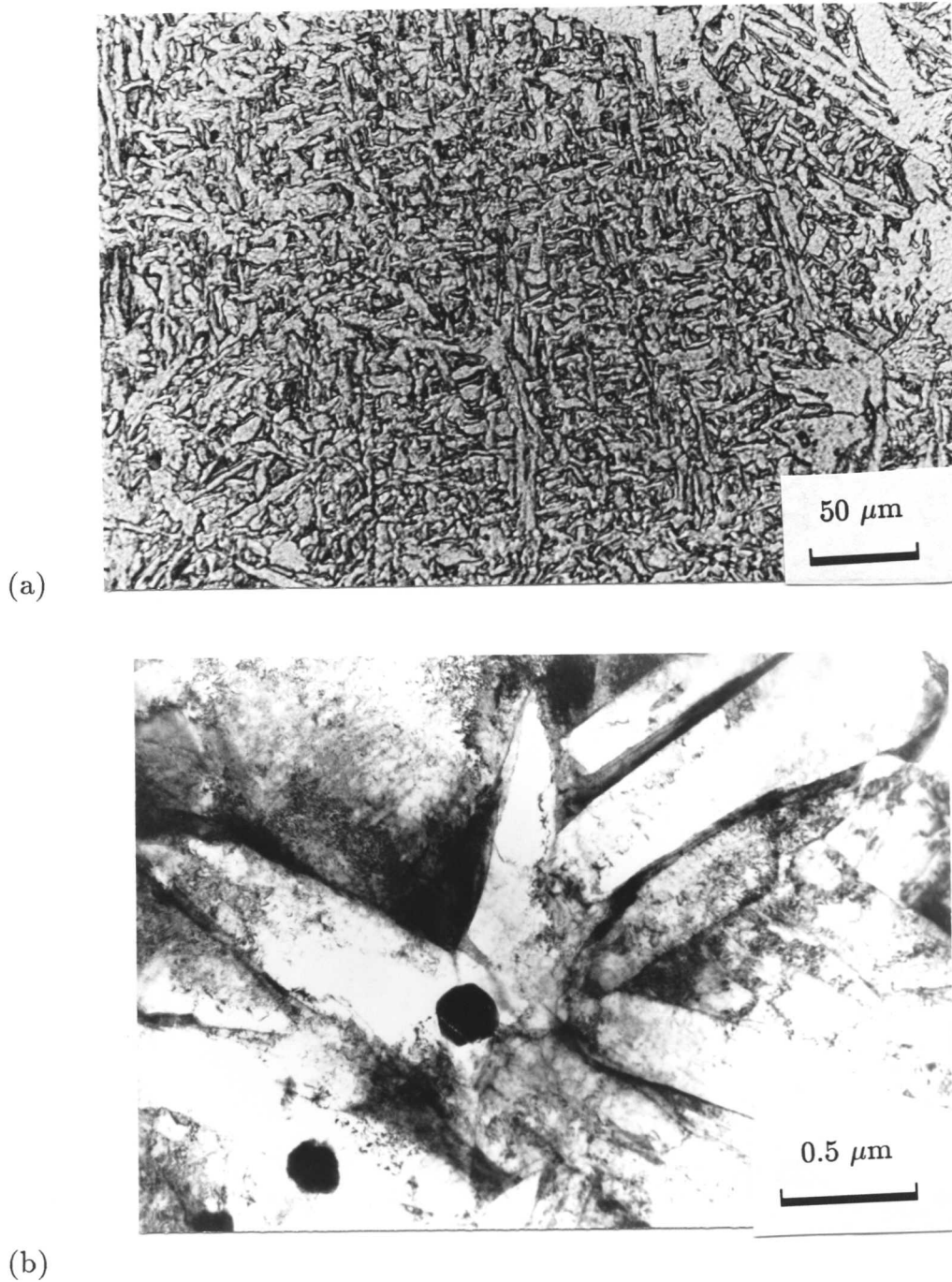
Fig. 1.16: *Micrographs showing acicular ferrite microstructure. (a) Optical micrograph of specimen from Fe-0.067-0.44Si-1.22Mn-0.01Mo-0.64Ni-0.39Cu (wt. %) weld deposit, isothermally transformed at 675 °C @ 50 s after austenitisation at 1000 °C @ 10 min. (b) TEM micrograph showing the inclusion assisted nucleation of acicular ferrite plates in Fe-0.06C-0.27Si-1.84Mn-2.48Ni-0.2Mo wt. % weld deposit, isothermally transformed at 460 °C @ 30 min after austenitisation at 1200 °C @ 30 min (after Yang, 1987).*

**1.9.4** *Martensite*

Martensite is a product of diffusionless transformation and can occur in the form of thin, lenticular plates, which often extend right across $\gamma$ grains, or as packets of approximately parallel, fine laths, whose size is generally less than that of the $\gamma$ grains. In both cases the parent and product crystals are related by an atomic correspondence and the formation of martensite causes the shape of the transformed region to change, this shape change is macroscopically an invariant-plane strain, the invariant-plane being the habit plane of martensite. The nucleation of martensite is generally athermal (but can be isothermal) and is believed to be diffusionless in nature. Martensite can occur at very low temperatures and its interface with the parent phase necessarily has to be glissile. Martensite forms at high undercoolings where the chemical free energy change for transformation is generally very large, well in excess of that required to accomplish diffusionless transformation even when the stored energy of the martensite is taken into account. Fig. 1.17 shows the formation of martensite in Fe-0.12C-0.3Si-0.5Mn-1.0Mo-2.5Cr (wt. %) alloy steel.



100 $\mu$m
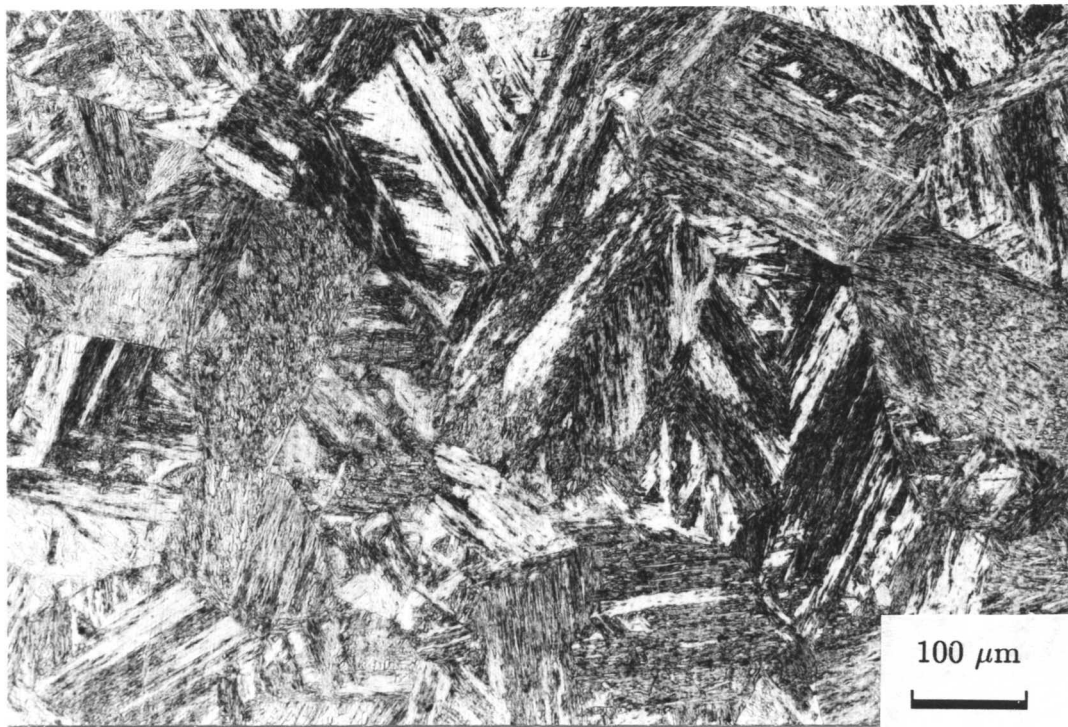
Fig. 1.17: *Micrographs showing martensite transformation in alloy of composition Fe-0.12C-0.3Si-0.5Mn-1.0Mo-2.5Cr (wt. %) steel quenched directly from 940 °C.*

## 1.10 Summary

A literature survey on some of the basic concepts of phase transformations in steels has been presented. The decomposition of austenite below the $Ae_3$ temperature can result in the formation of a varieties of reconstructive and displacive transformation products, which can be distinguished by the features such as shape deformation, thermodynamics, and morphology.

♣♣♣

# Chapter 2
## REAUSTENITISATION

The following chapter is a survey of the work in the published literature, on the formation of austenite, including an assessment of the kinetics of austenite formation.

### 2.1 General Introduction

The process of reaustenitisation is an important phenomenon and is of considerable industrial importance. It plays an important role in several methods involving the heat-treatment of steels. For example, the dual phase steels§ produced by intercritical annealing of low carbon alloy steels in the $\alpha + \gamma$ phase field to generate a mixture of ferrite and austenite, which is then quenched to induce martensitic transformation of the austenite (Fig. 2.1). Austenite formation is also important in many fabrication processes involving multipass welding. Although the growth of austenite during heating of steels above the eutectoid temperature was studied by Hultgren [1929], Roberts *et al.* [1943], Baeyertz [1942] many decades ago there is as yet no adequate theory on the reverse transformation from ferrite in quantitative terms.

The ferrite-martensite dual phase steels, which provide a good combination of strength and ductility have been extremely successful in producing dramatic reductions in the weight of cars. It has been shown that at a given tensile strength level, dual phase steels have superior formability to standard high strength low alloy (HSLA) steels [Hayami and Furukawa, 1975; Rashid and Rao, 1981]. Such steels are now used widely in the automobile industry because of their high strength to weight ratio, a desirable target in the automobile industry for the sake of fuel efficiency and performance.

There are two different approaches in the production of dual phase steels [Hayami *et al.* 1979]. One of them involves a combination of the accelerated cooling of austenite followed by slower cooling at around the ferrite transformation-start temperature $Ae_3$. This method provides the as hot-rolled dual phase steels

---

§ Dual phase steels consist of a strong phase 'martensite' as a load carrying constituent in a ductile ferrite matrix. The martensitic regions may be, in fact, contain some retained austenite and/ or lower bainite as well, depending on the chemical composition and the cooling rate of the steel [Rashid and Rao, 1981].
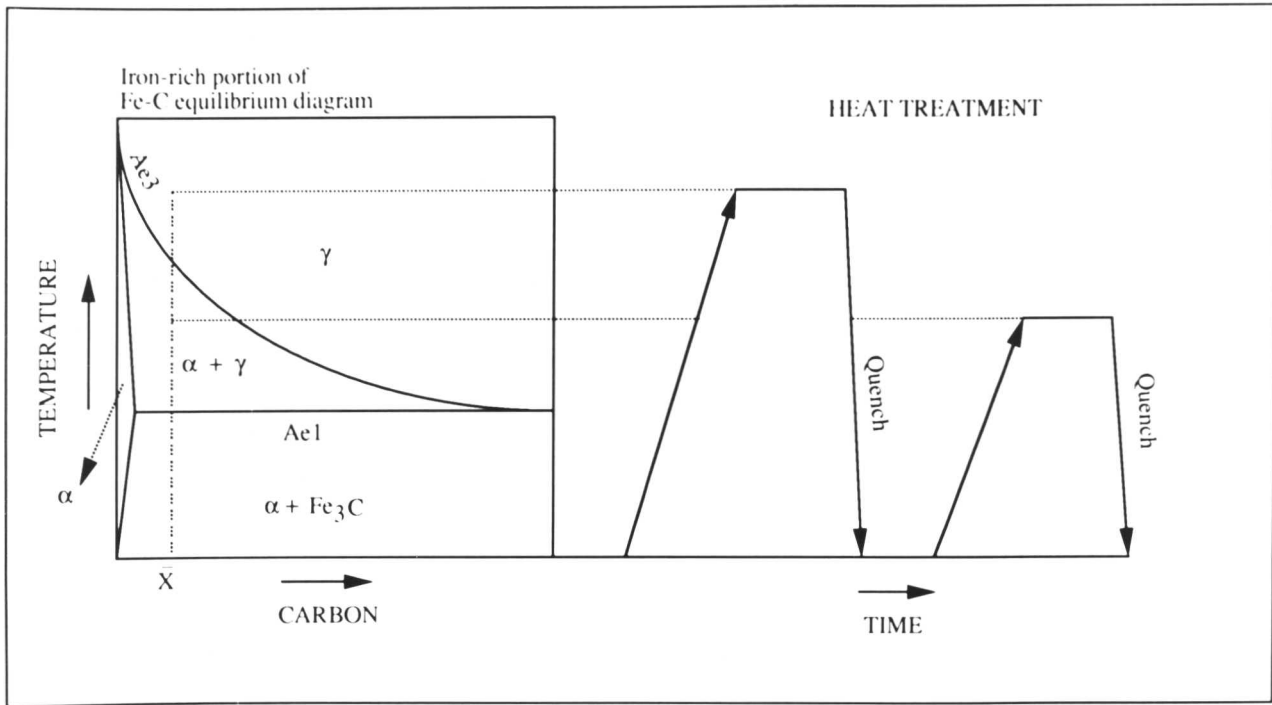
Fig. 2.1: *Schematic representation of heat treatments to produce dual phase steels.*

which are cheaper than those produced after cold rolling followed by intercritical annealing at temperatures between $Ae_1$ and $Ae_3$. In this latter heat treatment, a certain volume fraction of austenite, which has been produced by intercritical annealing, is surrounded by soft ferrite particles and the austenite then transformed into martensite during a final quenching process. In both processes, the amount, hardness and distribution of martensite, and the ferrite grain size determine the ultimate mechanical properties of the dual phase steel. The microstructure just before the final quench in the intercritical annealing method must therefore, be predicted precisely to achieve the optimum properties.

In multirun welds, the heat input associated with the deposition of successive layers of weld metal causes some or all of the underlying structure to be reheated to temperatures where austenite formation occurs [Yang and Bhadeshia, 1987a]. The new austenite then transforms again during cooling to a microstructure which is generally very different from the solidification structure associated with weld

deposits, and can seriously effect the mechanical properties of the final weld.

## 2.2 Effect of Initial Microstructure

The kinetics of reaustenitisation and the nature of the transformation products depend strongly on alloy chemistry, the initial microstructure and heating rate. A lot of research dealing with the initial microstructure effect on the morphology of austenite, has already been done [Baeyertz, 1942; Judd and Paxton, 1968; Law and Edmonds, 1980; Lenel and Honeycombe, 1984; Yang and Bhadeshia, 1987b; 1989; 1990; Yang, 1988]. The morphology of austenite may be divided roughly into two types; "acicular" and "globular". Some workers have further characterised the austenite as grain boundary allotriomorphic, sawteeth, grain boundary idiomorphs and Widmanstätten, morphologies, similar to the terminology common to the decomposition of austenite [Lenel and Honeycombe, 1984a; Plichta and Aaronson, 1974]. There is much less information on the transformation from the initial microstructure which is fully ferritic, or which contains a mixture of just bainitic ferrite and austenite, compared with other initial microstructures such as pearlite, a mixture of pearlite and ferrite and a mixture of carbides and martensite.

### 2.2.1 *Effect of Deformation on Austenite Formation*

Austenite formation in cold rolled steels is complicated by the recrystallisation of cold worked ferrite. Cold rolling serves to disperse and deform the pearlite, and the rapid spheroidisation of pearlitic cementite has occurred early in the intercritical annealing cycle [Yang *et al.* 1985]. Austenite forms on and around the spheroidised carbide particles, and the initial growth of austenite is accomplished by dissolution of carbide particles through the austenite to the austenite-ferrite interfaces.

Yang *et al.* [1985] showed that in cold rolled steels, austenite formed not only at ferrite boundaries but also within the ferrite grains. They also showed that austenite formed first on the boundaries between deformed and unrecrystallised ferrite grains and then on spheroidised cementite particles in recrystallised ferrite grains as illustrated in Fig. 2.2.

### 2.2.2 *Reaustenitisation from a Mixed Ferrite and Pearlite Microstructure*

The formation of austenite from a pearlitic microstructure was studied at an early stage in research on reaustenitisation [Hultgren, 1929; Baeyertz, 1942]. This work has been reviewed for application to ferrite-martensite dual phase steels. The nucleation of austenite in eutectoid steels has been reported to occur preferentially at the intersection of pearlite colonies [Roberts and Mehl, 1943].
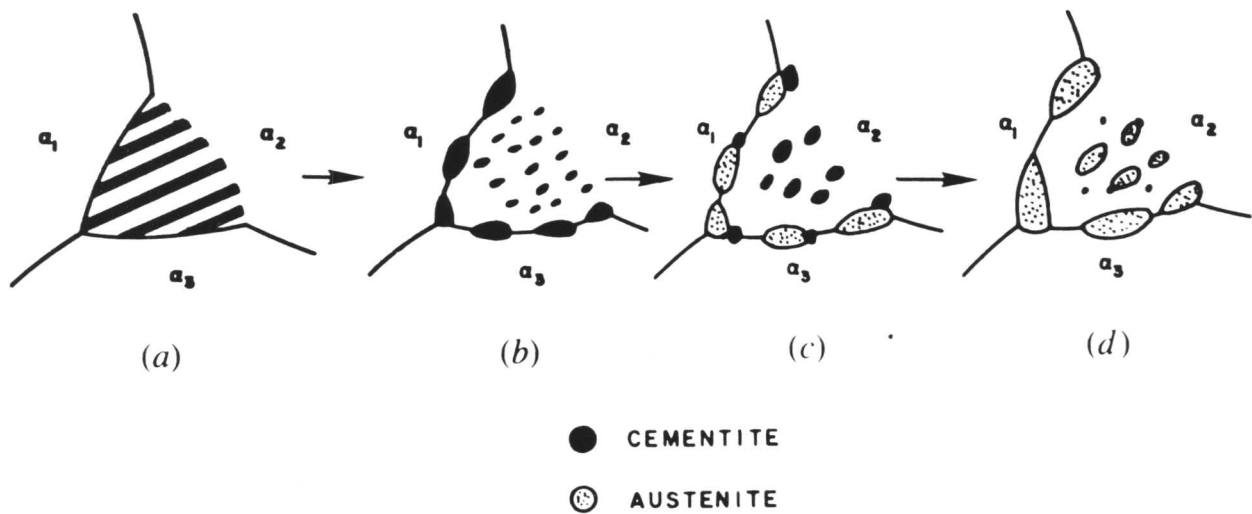
Fig. 2.2: *Schematic illustration of the austenite ($\gamma$ ) formation during low tempera-
ture intercritical annealing of a ferrite-pearlite microstructure [Speich et al. 1981].
a) Ferrite-pearlite starting structure. b) Spheroidisation of cementite and coarsen-
ing of cementite particles at $\alpha - \alpha$ boundaries. c) Nucleation of $\gamma$ at cementite
particles on $\alpha - \alpha$ boundaries. d) Nucleation of $\gamma$ on cementite particles within the
spheroidised pearlite colony and growth of austenite on $\alpha - \alpha$ boundaries.*

In spite of the large area per unit volume, the inter-lamellar surfaces do not seem
to act as the nucleation sites for austenite [Speich and Szirmae, 1969], although
a reasonable explanation for this is not yet available. In addition, the fact that
the formation of austenite is found to occur at the interfaces between ferrite grains
and pearlite colonies instead of at the inter-lamellar surfaces (in the case of the
mixture of ferrite and pearlite starting microstructure), suggests the importance of
ferrite-ferrite grain boundaries for the nucleation of austenite [Roberts and Mehl,

1943; Lenel and Honeycombe, 1984a; Speich and Szirmae, 1969; Cai *et al.* 1985 and Garcia and DeArdo, 1981]. Garcia *et al.* [1981] have studied the formation of austenite from a mixture of ferrite and pearlite and concluded that austenite appeared to nucleate on cementite particles which were located on either pearlite colony boundaries or boundaries separating pearlite colonies and ferrite grains. The same results have been reported by Speich *et al.* [1969] in the case of the formation of austenite in eutectoid steels.

**2.2.3** *Reaustenitisation from Ferrite and Spheroidised Cementite*

The mixture of ferrite and spheroidised cementite can be obtained by tempering martensite at a certain temperature. After tempering, most cementite particles tend to locate at the ferrite/ferrite grain boundaries instead of within the ferrite grains while in materials which have been tempered after cold working, most of the cementite particles are dispersed in the ferrite matrix away from the ferrite grain boundaries [Speich and Szirmae, 1969]. Using this technique, the role of cementite particles and ferrite grain boundaries for the nucleation and growth of austenite from a mixture of spheroidised cementite has been studied by several researchers [Judd and Paxton, 1968; Lenel and Honeycombe, 1984; Speich and Szirmae, 1969; Garcia and DeArdo, 1981]. In steels having a low number density of nucleation sites i.e., those which have few carbides at grain boundaries relative to the total amount of carbide, the growth of austenite will be controlled largely by the dissolution of carbides in ferrite ahead of the interface and diffusion of carbon through ferrite to the advancing interface. This produces Widmanstätten side-plates or sawteeth morphologies of austenite [Lenel and Honeycombe, 1984a].

Yang *et al.* [1985; 1985b] have studied the formation of austenite from ferrite-spheroidised cementite microstructures. They showed that the spheroidisation of cementite particles plays an important role in the development and distribution of austenite during low temperature intercritical annealing. Austenite forms on and around the spheroidised carbide particles, and that the initial growth of austenite is accomplished by the dissolution of cementite particles and the diffusion of carbon from the particles through the austenite to austenite-ferrite interfaces. This process directly led them to the distribution of austenite at grain boundary allotriomorphs and intragranular idiomorphs in specimens intercritically annealed at low temperatures. Nehrenberg [1950] noticed that "acicular" austenite grains developed from spheroidised ferrite/cementite structures only if they were produced from martensite rather than pearlite. Dirnfeld *et al.* [1974] have studied the formation of austenite

in a fine grained tool steel. They demonstrated that nucleation starts at carbides which lie at the ferrite grain boundaries.

**2.2.4** *Reaustenitisation from Martensitic Microstructures*

Recently a number of investigators have examined in detail the formation of austenite from martensite in low carbon steels. Both acicular and globular austenite morphologies were observed [Kinoshita and Ueda, 1974; Matsuda and Okamura, 1974; Matsuda and Okamura, 1974; Homma, 1974, Watanabe and Kunitake, 1975]. It is generally agreed that acicular austenite is inherited initially from the elongated nature of the prior martensite laths and/ or packets, and is favoured by slow heating rates [Kinoshita and Ueda, 1974; Matsuda and Okamura, 1974; Matsuda and Okamura, 1974], low austenitising temperatures and acicular starting microstructures, such as tempered martensite, where lath boundaries are well decorated by carbide precipitates [Homma, 1974; Watanabe and Kunitake, 1975]. It has also been demonstrated that each acicular austenite grain formed from ferrite laths with the same orientation has the same crystallographic orientation and has the Kurdjumov-Sachs (K-S) orientation relation with the ferrite [Watanabe and Kunitake, 1975]. In the later stages of the transformation, more acicular austenite grains were forced to nucleate within the ferrite regions and eventually the austenite grains coalesce to assume a globular morphology.

Reaustenitisation of martensite has been studied in ferrite-martensite dual phase steels which are obtained by intercritical annealing followed by quenching to ambient temperature to get the appropriate mixture of ferrite and martensite. Nucleation of austenite occurs preferentially at the prior austenite grain boundaries [Baeyertz, 194; Matsuda and Okamura, 1974; Homma, 1974; Law and Edmonds, 1980]. Acicular austenite forms within the prior austenite grains of the martensitic, bainitic structures, and the grains soon coalesce to form globular austenite grains [Law and Edmonds, 1980; Watanabe and Kunitake, 1975; Watanabe and Kunitake, 1975]. Watanabe *et al.* [1975] studied reaustenitisation from martensite microstructure in two types of steels, Fe-0.13C-0.25Si-0.76Mn-0.19Cu-0.98Ni-0.5Cr-0.51Mo and Fe-0.40C-0.12Si-9.16Ni (wt. %). They found that austenite formed with an acicular shape with each acicular austenite grain having the same orientation, the Kurdjumov-Sachs relationship with the ferrite. Law *et al.* [1980] found that austenite allotriomorphs nucleated on ferrite grain boundary bear a K-S orientation relationship to one of the ferrite grains, and grow into the adjacent grain by the migration of an incoherent interface.

**2.2.5** *Reaustenitisation from Ferrite*

Little work has been done on reaustenitisation of ferritic samples because of the extremely low hardenability of these steels, which makes it almost impossible to freeze the austenite microstructure to ambient temperature even in the form of martensite phase. Speich *et al.* [1969] studied the formation of austenite in low carbon steel using laser-pulse heating and a helium-water droplet spray technique which allows $10^6$ $^{o}$C s$^{-1}$ of heating rate and $10^5$ $^{o}$C s$^{-1}$ of cooling rate. They showed that the formation of austenite had occurred at the ferrite/ferrite grain boundaries where they found fine ferrite grains transformed from austenite which grew during the rapid heat treatment.

**2.2.6** *Reaustenitisation from Bainitic Ferrite*

A little work has been reported in the past dealing with the formation of austenite from bainitic microstructures including acicular ferrite. The formation of austenite from bainitic microstructures has been studied by Nehrenberg, [1950]; Matsuda *et al.* [1974a, 1974b]; Matsuda and Okamura, [1974], Law *et al.* [1980], Yang *et al.* [1987]; Yang, [1988]; Yang *et al.* [1989] Yang and Bhadeshia, [1990]. Law *et al.* [1980] have reported that the nucleation of austenite had occurred primarily at the prior austenite grain boundaries and that site saturation occurred after rapidly. Isothermal reaustenitisation at high temperatures seemed to lead more intragranular nucleation of austenite.

Recently, Yang and Bhadeshia, [1987, 1989] and Yang, [1988] have investigated the growth of austenite from bainite and acicular ferrite. They studied isothermal and continuous heating transformations from upper bainite and acicular ferrite in a matrix of austenite. The starting microstructures thus already contained austenite, whose nucleation is consequently unnecessary during heating. With isothermal transformation, they found that reverse transformation did not happen immediately the temperature was raised above that at which the bainite or acicular ferrite had formed, even though the alloy was within the intercritical region of the phase diagram. They modelled the growth of austenite in terms of one dimensional carbon diffusion-controlled movement of planar austenite/ferrite interfaces, as shown in Fig. 2.3.